CD300lf is the primary physiologic receptor of murine norovirus but not human norovirus

Vincent R. Graziano[1], Forrest C. Walker[2], Elizabeth A. Kennedy[2], Jin Wei[1], Khalil Ettayebi[6], Madison S. Simões[1], Renata B. Filler[1], Ebrahim Hassan[2], Leon L. Hsieh[3], Abimbola O. Kolawole[4], Christiane E. Wobus[4], Lisa C. Lindesmith[5], Ralph S. Baric[5], Mary K. Estes[6], Robert C. Orchard[7], Megan T. Baldridge[2]*, and Craig B. Wilen[1]*

[1]Departments of Laboratory Medicine and Immunobiology, Yale University School of Medicine, New Haven, CT, USA

[2]Department of Medicine, Division of Infectious Diseases, Edison Family Center for Genome Sciences & Systems Biology, Washington University School of Medicine, Saint Louis, MO, USA

[3]Department of Molecular Microbiology and Immunology, Bloomberg School of Public Health, Johns Hopkins University, Baltimore, MD, USA

[4]Department of Microbiology and Immunology, University of Michigan Medical School, Ann Arbor, Michigan, USA.

[5]Department of Epidemiology, University of North Carolina, Chapel Hill, NC, USA

[6]Departments of Medicine and Molecular Virology & Microbiology, Baylor College of Medicine, Houston, TX, USA

[7]Department of Immunology, University of Texas Southwestern Medical School, Dallas, TX, USA

*To whom correspondence should be addressed: craig.wilen@yale.edu, mbaldridge@wustl.edu

Abstract

Murine norovirus (MNoV) is an important model of human norovirus (HNoV) and mucosal virus infection more broadly. Viral receptor utilization is a major determinant of cell tropism, host range, and pathogenesis. The *bona fide* receptor for HNoV is unknown. Recently, we identified CD300lf as a proteinaceous receptor for MNoV. Interestingly, its paralogue CD300ld was also sufficient for MNoV infection *in vitro*. Here we explored whether CD300lf is the sole physiologic receptor *in vivo* and whether HNoV can use a CD300 ortholog as an entry receptor. We report that both CD300ld and CD300lf are sufficient for infection by diverse MNoV strains *in vitro*. We further demonstrate that CD300lf is essential for both oral and parenteral MNoV infection and to elicit anti-MNoV humoral responses *in vivo*. In mice deficient in STAT1 signaling, CD300lf is required for MNoV-induced lethality. However, after high dose intraperitoneal challenge with MNoV in *Cd300lf*$^{-/-}$*Stat1*$^{-/-}$ mice a single amino acid mutation in the MNoV capsid protein emerged. This substitution did not alter receptor utilization *in vitro*. Finally, we demonstrate that human CD300lf (huCD300lf) is not essential for HNoV infection, nor does huCD300lf inhibit binding of HNoV virus-like particles to glycans. Thus, we report huCD300lf is not a receptor for HNoV.

Author Summary

Human norovirus is the leading cause of non-bacterial gastroenteritis causing up to 200,000 deaths each year. How human norovirus enters cells is unknown. Because human norovirus is difficult to grow in the laboratory and in small animals, we use mouse or murine norovirus as a model system. We recently discovered that murine norovirus can use the either CD300ld or CD300lf as a receptor *in vitro*. We also showed that CD300lf deficient mice were resistant to oral challenge with a single virus strain. Here we determined that CD300lf is essential for infection of diverse murine norovirus strains in cell lines and in mice with normal immune systems demonstrating it's the primary physiologic receptor for diverse murine norovirus strains independent of infection route. However, in immunodeficient mice injected with high dose virus directly into the abdominal cavity, we observed a norovirus mutant that enabled CD300lf-independent infection. Finally, we demonstrated that human CD300lf is not the elusive receptor for human norovirus.

Introduction

Human norovirus (HNoV) is the leading cause of infectious gastroenteritis globally, yet our understanding of how HNoV enters cells is limited[1-4]. Viral entry is the first and often rate-limiting step of the viral life cycle and is a major determinant of cell tropism, species range, host genetic susceptibility, and pathogenesis[1,5]. Entry includes virion attachment to the host cell membrane, receptor engagement, internalization, and genome release into the cell cytoplasm[1,5]. Both histo-blood group antigens (HBGAs) and bile salts bind HNoV and promote infection[6-8]. The identity of a proteinaceous cellular receptor(s) for HNoV remains unknown[1,8,9].

Murine norovirus (MNoV) represents a surrogate animal model for studies of HNoV infection and pathogenesis[1,10,11]. In contrast to HNoV, diverse infectious molecular clones exist for MNoV that can be readily propagated both *in vitro* and in mice. MNoV and HNoV share similar genome and capsid architecture, fecal-oral transmission routes, interactions with bile salts, and the ability to cause both acute and persistent infection[1,7,8,10-14]. Recently, we identified CD300 family members CD300ld and CD300lf as functional receptors for MNoV[15,16]. CD300lf is necessary for infection of MNoV-susceptible RAW 264.7 and BV2 cell lines while both CD300ld and CD300lf are sufficient to confer susceptibility to cell lines from different species when ectopically expressed[15,16]. In addition, CD300lf-deficient mice are resistant to fecal-oral transmission of MNoV strain CR6 ($MNoV^{CR6}$)[15]. Whether CD300lf is essential for genetically diverse MNoV strains, parenteral infection routes, or in the setting of immunodeficiency is unclear. Finally, it is unknown whether human CD300lf functions as a receptor for HNoV.

Noroviruses are non-enveloped, positive-sense single-stranded RNA viruses[1]. The viral capsid exhibits T=3 icosahedral symmetry and is comprised of 90 dimers of the

major structural protein VP1[17]. VP1 contains a shell (S) domain and a protruding (P) domain that contains a proximal P1 and distal P2 subdomain[18]. P2 is the target for several neutralizing monoclonal antibodies for both HNoV and MNoV and contains the receptor binding site for MNoV[12,13]. Co-crystal structures and mutagenesis studies have identified that the CC' and CDR3 loops of CD300lf directly bind to a cleft between the AB' and DE' loops of the MNoV VP1 P2 subdomain[13,15,19]. Each CD300lf binds one P2 monomer, albeit at relatively low affinity, suggesting that norovirus-receptor interactions are largely driven by avidity[13]. Interestingly, binding of MNoV to CD300lf is promoted by both divalent cations and bile salts[12,13,15].

Diverse MNoV strains have been described with distinct pathogenic properties[20-22]. Specifically, $MNoV^{CW3}$ causes acute systemic infection that is cleared by the adaptive immune system, while there are other strains including $MNoV^{CR6}$ that cause chronic enteric infection that can last for months if not the life of the animal[20,23]. Interestingly, a single amino acid in the P2 domain of MNoV VP1 is sufficient to confer lethality in mice deficient in type I interferon signaling, suggesting a role for virus-receptor interactions in determining pathogenesis[20,24].

There are eight CD300 family members in mice and seven in humans, each containing a conserved ectodomain, a single transmembrane domain, and a more variable cytoplasmic signaling domain[25,26]. The ectodomains bind diverse phospholipids found on dead and dying cells, resulting in activating or inhibitory signals depending upon the cellular and molecular context[26-30]. Both CD300ld and CD300lf are expressed in diverse myeloid cells, while CD300lf is additionally expressed in lymphoid cells and rare intestinal epithelial cells called tuft cells, which are the primary target cell of $MNoV^{CR6}$ [25,31].

Here we show that CD300lf is essential for fecal-oral transmission and pathogenesis of diverse MNoV strains in both immunocompetent and immunodeficient mice, suggesting CD300lf is the primary physiologic receptor for MNoV. We also identify CD300lf-independent viral infection in the setting of extra-intestinal challenge in immunodeficient mice, suggesting a potential role for CD300ld or other receptors in this non-physiological infection route. Finally, we demonstrate that CD300lf and related CD300 family members do not function as HNoV receptors.

Results

HNoV induces vomiting and diarrhea within approximately 24 hours after infection[32-34]. In contrast, MNoV replicates to high titers but is largely avirulent in immunocompetent mice [10,35,36]. Diverse strains of MNoV have been described that can cause either acute self-limiting infection (e.g. MNoV^{CW3}) or chronic infection (e.g. MNoV^{CR6}) in wild type mice[20,21]. We previously demonstrated that *Cd300lf*$^{-/-}$ mice do not shed detectable MNoV^{CR6} between 3 and 21 days post-oral challenge; however, the role of CD300lf during earlier time points and in systemic tissues is unclear[15]. MNoV^{CW3} is an infectious molecular clone derived from the MNV-1 plaque isolate CW3[14,20]. MNoV^{CW3} can infect myeloid and lymphoid cells in the intestine and secondary lymphoid organs and can cause lethal infection in mice deficient in type I interferon signaling[14,20,37,38]. To test whether CD300lf was essential for MNoV^{CW3} infection *ex vivo*, we challenged bone marrow-derived macrophages (BMDMs) from *Cd300lf*$^{+/-}$ or *Cd300lf*$^{-/-}$ mice with MNoV^{CW3}. *Cd300lf*$^{-/-}$ BMDMs did not produce infectious virus as measured by plaque assay (Fig 1A) nor did they express the MNoV non-structural protein NS1/2 as detected by flow cytometry (Fig 1B-C). CD300lf is thus

essential for MNoV^{CW3} infection of murine BMDMs. To test the role of CD300lf *in vivo*, we challenged *Cd300lf*$^{+/-}$ and *Cd300lf*$^{-/-}$ littermate mice with 10^6 plaque forming units (PFU) of MNoV^{CW3} perorally (PO) and measured infectious virus by plaque assay (Fig 1D) and viral genomes by qPCR (Fig 1E). At 24 hours post-infection (hpi), infectious virions were undetectable in *Cd300lf*$^{-/-}$ mice in the mesenteric lymph node (MLN), ileum, and colon, in contrast to *Cd300lf*$^{+/-}$ littermates. At this dose and time point, MNoV^{CW3} was not detected in the spleen of control or knockout mice. Viral genomes were similarly undetectable in *Cd300lf*-deficient animals (Fig 1E).

Next, we asked whether CD300lf was required for infection by genetically diverse MNoV strains. MNoV strains are derived from a single genogroup (Genogroup V) and alignments of MNoV VP1 previously revealed at least five distinct clusters, from which we selected representative strains MNoV^{CW3}, MNoV^{CR6}, MNoV^{WU23}, MNoV^{CR3}, and MNoV^{CR7} (Table 1) [21,39-41]. An alignment of strains highlights the broad amino acid conservation of the capsid protein, including the CD300lf binding sites, and bile-acid interacting sites described previously (Fig S1)[13]. Among these strains, there is no variability in the 11 VP1 residues shown to interact with the secondary bile salts glycochenodeoxycholic acid (GCDCA) or lithocholic acid (LCA)[13]. However, there is variation in 4 of the 17 VP1 residues previously shown to interact with CD300lf, suggesting diverse strains may utilize receptors other than CD300lf (Fig S1)[13]. To test the hypothesis that diverse MNoV strains differentially utilize CD300lf, we first tested whether CD300lf was necessary and sufficient for infection by these strains *in vitro*. We challenged CD300lf-deficient BV2 microglial cells with six diverse MNoV strains. All strains induced cell death in wild-type BV2 cells but not CD300lf-deficient cells,

151 demonstrating CD300lf is essential for virus induced-lethality in BV2 cells (Fig 2A).
152 Next, we asked whether CD300ld and CD300lf are sufficient to confer susceptibility to
153 human HeLa cells. Consistent with our prior findings, both CD300ld and CD300lf are
154 sufficient for infection by MNoV^{CW3} as measured by expression of the MNoV non-
155 structural protein NS1/2 by flow cytometry[15]. Similarly, both CD300ld and CD300lf are
156 sufficient for MNoV^{WU23}, MNoV^{CR3}, MNoV^{CR7}, MNoV^{MNV3}, and MNoV^{S99} infection (Fig
157 2B). All tested MNoV strains utilize CD300ld and CD300lf at similar efficiencies when
158 overexpressed in HeLa cells.

159 To determine whether CD300lf was essential for infection *in vivo*, we challenged
160 *Cd300lf*$^{+/-}$ and *Cd300lf*$^{-/-}$ littermates with 10^6 PFU PO of either MNoV^{CW3}, MNoV^{CR6},
161 MNoV^{WU23}, MNoV^{CR3}, or MNoV^{CR7} for seven days. These viruses represent each of the
162 five distinct MNoV VP1 phylogenetic clusters described previously[39]. MNoV^{CW3} causes
163 acute systemic infection that is cleared by 10-14 days post-infection (dpi), while
164 MNoV^{CR6}, MNoV^{CR3}, and MNoV^{CR7} cause persistent infection[21]. The *in vivo*
165 characteristics of MNoV^{WU23} are uncharacterized[21]. Consistent with prior studies, we
166 observed differential tissue tropism associated with different MNoV strains[21]. In control
167 mice, viral genomes for all tested MNoV strains were shed in the feces of some mice
168 with the exception of MNoV^{CW3} (Fig 2C). All tested MNoV strains were detected in the
169 MLN (Fig 2D). All strains were detectable albeit at varying levels in the ileum and colon.
170 Interestingly, only MNoV strains MNoV^{CW3} and MNoV^{WU23} were detectable in the
171 spleen. MNoV^{CR6}, MNoV^{CR3}, and MNoV^{CR7}, which are known to establish chronic
172 infection in immunocompetent mice did not have detectable viral genomes in the
173 spleen. MNoV genomes were not detected in any tissue (MLN, spleen, ileum, colon, or

174 feces) of any *Cd300lf*-deficient mice challenged with any of the five MNoV strains (Fig
175 2C-G). To determine whether there was MNoV infection below the limit of detection, we
176 collected feces from *Cd300lf*$^{+/-}$ or *Cd300lf*$^{-/-}$ mice challenged with MNoV^{CR6} seven days
177 prior, and then gavaged the feces into *Stat1*$^{-/-}$ recipient mice which lack innate immunity
178 and are exquisitely sensitive to MNoV infection[14,15]. Seven days after fecal gavage we
179 detected MNoV^{CR6} in *Stat1*$^{-/-}$ mice challenged with feces from *Cd300lf*$^{+/-}$ mice but not
180 from *Cd300lf*$^{-/-}$ mice (Fig 2H). These results suggest CD300lf is critical for infection by
181 multiple MNoV strains in immunocompetent mice *in vivo*.

182 To further determine whether CD300ld or an alternative receptor was sufficient
183 for MNoV infection below our limit of detection, we assessed the humoral immune
184 response against MNoV^{CW3} at 14 days dpi, a time point after viral clearance by the
185 adaptive immune system. A 1:10 dilution of sera from *Cd300lf*$^{+/-}$ mice that cleared
186 MNoV^{CW3} infection neutralized MNoV^{CW3} *in vitro* as measured by BV2 cell viability (Fig
187 3A). The IC_{50} from *Cd300lf*$^{+/-}$ mice was approximately 1:80 in contrast to sera from
188 *Cd300lf*$^{-/-}$ mice which did not reach an IC_{50} (Fig 3B). To determine whether MNoV^{CW3}
189 elicited a non-neutralizing humoral response in *Cd300lf*$^{-/-}$ mice, we measured anti-
190 MNoV IgG and IgM in the sera. *Cd300lf*$^{+/-}$ mice had a significantly higher anti-MNoV
191 IgG and IgM response consistent with resistance of *Cd300lf*$^{-/-}$ mice to MNoV^{CW3}
192 infection (Fig 3C-D).

193 Next, we asked whether CD300lf was essential for fecal-oral transmission of
194 MNoV^{CW3} in *Stat1*$^{-/-}$ mice. We challenged *Cd300lf*$^{+/+}$, *Cd300lf*$^{+/-}$ or *Cd300lf*$^{-/-}$ mice on a
195 *Stat1*$^{-/-}$ background with 10^6 PFU MNoV^{CW3} PO, which is greater than 1000-fold above
196 the lethal dose[15]. All *Cd300lf*$^{+/+}$*Stat1*$^{-/-}$ succumbed to lethal infection by five dpi (Fig 4A).

197 *Cd300lf*$^{+/-}$*Stat1*$^{-/-}$ similarly all died but with a one-day delay in death suggesting a
198 modest CD300lf gene dosage effect on MNoV pathogenesis. In contrast, all ten
199 *Cd300lf*$^{-/-}$*Stat1*$^{-/-}$ mice survived until at least 21 dpi without overt clinical manifestations
200 (Fig 4A).

201 Given the distinct target cell types, tissue tropism, and pathogenesis between
202 MNoV strains, we next tested whether *Cd300lf*$^{-/-}$*Stat1*$^{-/-}$ mice were susceptible to
203 MNoV^{CR6} infection. In contrast to MNoV^{CW3}, MNoV^{CR6} is not lethal in *Stat1*$^{-/-}$ mice
204 although the virus replicates to higher titers and can spread to extra-intestinal tissues[14].
205 All *Cd300lf*$^{+/+}$*Stat1*$^{-/-}$ and *Cd300lf*$^{+/-}$*Stat1*$^{-/-}$ mice challenged with 10^6 PFU PO MNoV^{CR6}
206 survived the seven-day infection. Viral genomes were detected in the feces, MLN,
207 spleen, ileum, and colon (Fig 4B-F). There was a modest CD300lf gene dosage effect
208 in the spleen ($p<0.05$) among *Cd300lf*$^{+/+}$ and *Cd300lf*$^{+/-}$ mice, but this was not
209 statistically significant in the MLN, ileum, colon, or feces (Fig 4C-F). Relative to *Stat1*$^{+/+}$
210 mice, viral genome copies were elevated and extra-intestinal spread to the spleen was
211 observed consistent with prior findings (Fig 2C-G). Importantly, *Cd300lf*$^{-/-}$*Stat1*$^{-/-}$ mice
212 were resistant to MNoV^{CR6} in all tissues examined. Two *Cd300lf*$^{-/-}$*Stat1*$^{-/-}$ mice had
213 detectable viral genomes in the MLN but not in other tissues (Fig 4C). A third mouse
214 had detectable low-level viral RNA in the colon but not in any other tissue, possibly
215 reflective of input virus or a false positive (Fig 4F).

216 The natural defenses of the gastrointestinal mucosa represent a bottleneck to
217 viral infection. To test whether CD300lf was essential for parenteral infection routes, we
218 bypassed the gastrointestinal tract by administering 10^7 PFU MNoV^{CW3} intraperitoneally
219 (IP) to *Cd300lf*$^{-/-}$*Stat1*$^{-/-}$ mice. All *Cd300lf*$^{+/+}$*Stat1*$^{-/-}$ and *Cd300lf*$^{+/-}$*Stat1*$^{-/-}$ mice died by

five or six dpi, respectively (Fig 5A). Two of nine *Cd300lf*$^{-/-}$*Stat1*$^{-/-}$ mice died at 10 and 14 dpi with the remaining mice surviving at least 21 days. The two *Cd300lf*$^{-/-}$*Stat1*$^{-/-}$ mouse deaths were observed in independent experiments. Virological data was not available from these animals; therefore, whether MNoV^{CW3} contributed to the death of these two *Cd300lf*$^{-/-}$*Stat1*$^{-/-}$ mice is unknown.

Next, we challenged mice with 10^7 PFU MNoV^{CR6} IP. In contrast to the lower-dose MNoV^{CR6} administered PO, 77% (7/9) of *Cd300lf*$^{+/+}$*Stat1*$^{-/-}$ mice and 66% (2/3) *Cd300lf*$^{+/-}$*Stat1*$^{-/-}$ mice died (Fig 5B). All six *Cd300lf*$^{-/-}$*Stat1*$^{-/-}$ mice survived IP infection with 10^7 MNoV^{CR6} until sacrifice at seven dpi. Interestingly, MNoV^{CR6} genomes were detected in the MLN, spleen, ileum, and colon of *Cd300lf*$^{-/-}$*Stat1*$^{-/-}$ mice (Fig 5C). MNoV^{CR6} from *Cd300lf*$^{-/-}$*Stat1*$^{-/-}$ mice infected with 10^7 PFU MNoV^{CR6} IP was Sanger sequenced, revealing a single nucleotide change (T6595A) resulting in a phenylalanine to isoleucine mutation at position 514 (F514I) in the P1 domain of VP1 (Supplemental Table 1). This mutation was detected in the spleen, ileum, and colon from two different mice. Thus, while CD300lf is essential for MNoV infection by oral inoculation in immunocompetent hosts, CD300lf-independent replication of MNoV may occur under high-dose IP challenge in *Stat1*$^{-/-}$ mice.

To determine whether the F514I variant observed enabled CD300lf-independent infection, we generated an infectious molecular clone containing this mutation on the MNoV^{CR6} background (MNoV^{F514I}). Similar to MNoV^{CR6}, MNoV^{F514I} was cytotoxic to WT BV2 cells but did not affect cell viability in *Cd300lf*-deficient BV2 cells, demonstrating this mutation did not enable alternative receptor utilization in BV2 cells (Fig 6A). We then asked whether MNoV^{F514I} could preferentially utilize CD300ld relative to CD300lf

when ectopically expressed in HeLa cells. MNoV^{F514I} and MNoV^{CR6} were both able to utilize CD300ld and CD300lf at similar ratios when overexpressed suggesting this mutation does not enhance CD300ld utilization *in vitro* (Fig 6B). Next, we thermally stressed MNoV^{CR6}, MNoV^{F514I}, MNoV^{CW3} to probe differences in virion stability as mutations that confer heat resistance were recently demonstrated to alter the VP1 conformation and thus may affect receptor utilization[42]. MNoV^{F514I} and MNoV^{CR6} had similar thermal stability (Fig 6C). Interestingly, this was increased relative to MNoV^{CW3} (Fig 6C). To investigate whether MNoV^{F514I} altered receptor utilization *in vivo*, we challenged *Cd300lf*$^{+/-}$ or *Cd300lf*$^{-/-}$ mice with 10^6 PFU MNoV^{F514I} PO. MNoV^{F514I} readily infected *Cd300lf*$^{+/-}$ mice and maintained similar tissue tropism as the parental MNoV^{CR6} (Fig 6D-G). Also similar to MNoV^{CR6}, MNoV^{F514I} genomes were not detectable in the MLN, spleen, ileum, colon, or feces of CD300lf$^{-/-}$ mice suggesting MNoV^{F514I} is not sufficient to alter receptor utilization in immunocompetent mice when administered PO (Fig 6D-H).

Next, given the structural and genetic similarity between MNoV and HNoV, we tested whether human CD300lf (huCD300lf) is a receptor for HNoV. First, we assessed the ability of huCD300lf to prevent binding of recombinant HNoV virus-like particles (VLPs) to HBGAs in pig gastric mucin. To increase the avidity of the potential CD300lf and VLP interaction, we generated Fc-fusion proteins with the either huCD300lf or human CD300ld (huCD300ld) ectodomains. We recently demonstrated that an Fc-fusion protein of mouse CD300lf has substantially increased binding and neutralizing ability on MNoV[13]. We incubated HNoV VLPs with 10 µg/ml of either Fc-huCD300lf, Fc-huCD300ld, or a buffer-only control and measured HBGA-bound VLPs by ELISAs.

Neither Fc-huCD300lf or Fc-huCD300ld inhibited binding of GI.1 Norwalk, GI.3 Desert Shield Virus, GII.4 1997, or GII.4 2012 VLPs to HBGAs (Fig 7A)[43,44]. Next, we asked whether potential HNoV interactions with huCD300lf were necessary for infection of human intestinal enteroids (HIEs). Differentiated monolayers of HIEs were incubated with polyclonal anti-huCD300lf or an IgG1 control and then challenged with HNoV GII.4 from stool filtrate. Anti-huCD300lf had no effect on HNoV genome replication at 24 hpi relative to the isotype control (Fig 7B). Finally, we asked whether Fc-huCD300lf could neutralize HNoV GII.4. Virus was pre-incubated with up to 50 µg/ml of Fc-huCD300lf and then used to infect HIEs. Fc-huCD300lf did not affect viral genome replication relative to a control protein (Fig 7C). Together these data indicate that huCD300lf is not a receptor for HNoV.

Discussion

Here we demonstrate that CD300lf, and not CD300ld, is the primary physiologic receptor for diverse MNoV strains *in vivo*. We demonstrated that CD300lf is essential for detectable viral infection at multiple time points with diverse MNoV strains as measured by plaque assay, qPCR, and serologic response. Interestingly, both CD300ld and CD300lf are sufficient to mediate MNoV entry when ectopically expressed *in vitro* yet CD300ld is not sufficient for oral or parenteral transmission in immunocompetent mice. Several possibilities may explain this discordance. First, CD300ld receptor utilization has only been described when overexpressed at supraphysiologic levels[15,16]. Similarly the soluble recombinant ectodomain of CD300lf can neutralize MNoV infection in contrast to that of CD300ld[15]. This raises the possibility that CD300ld utilization by MNoV is inefficient

289 relative to CD300lf and that our overexpression assays are not sufficiently sensitive to
290 quantify differences in receptor utilization efficiency. A similar phenomenon has been
291 described with HIV-1, which can engage co-receptors other than CCR5 and CXCR4 when
292 overexpressed in cell lines, but not under physiologically relevant conditions[45,46]. Second,
293 CD300ld and CD300lf have overlapping yet distinct cell type expression, raising the
294 possibility that CD300ld-expressing cells are either not permissive to MNoV because of
295 a post-entry restriction or because CD300ld-expressing cells are not anatomically
296 accessible to MNoV. Consistent with this, intestinal tuft cells, which are the major target
297 of MNoV^{CR6} in the intestines, express CD300lf but not CD300ld[31,47].

298 Although we demonstrated that *Cd300lf*-deficient mice are resistant to diverse
299 MNoV strains via both oral and parenteral routes, we observed detectable viral genomes
300 in *Cd300lf*$^{-/-}$*Stat1*$^{-/-}$ mice inoculated with high-dose MNoV^{CR6} IP, consistent with CD300lf-
301 independent viral replication. Sanger sequencing of virus from tissues from multiple mice
302 revealed a single amino acid mutation (F514I) in the P1 domain of MNoV VP1.
303 Surprisingly, CD300lf remained essential for MNoV^{F514I} infection both *in vitro* and in
304 immunocompetent mice, raising the question as to why this viral variant emerged and
305 whether it has physiologic relevance. One possibility is that MNoV^{F514I} enables the virus
306 to better utilize CD300ld, or an unknown alternative receptor *in vivo*, but only in a *Stat1*-
307 deficient background. Defects in innate immunity may enable broader cell tropism due to
308 removal of post-entry viral restriction, thus permitting CD300lf-independent replication *in*
309 *vivo*. The molecular consequences of F514I are intriguing in that this mutation is on the
310 opposite side of the P domain from the receptor binding site, suggesting an allosteric
311 mechanism of receptor regulation. One such mechanism could be altering the

312 "breathability" of the P domain, which is connected to the capsid shell by a flexible
313 linker[12,48]. Bile salts both increase MNoV-receptor binding and induce collapse of the P
314 domain onto the shell[12]. Whether F514I has a similar effect remains an important future
315 direction.

316 The physiologic function of CD300lf is as a cell death sensor and
317 immunoregulatory protein[25]. Interestingly, the CD300 locus is under positive selection and
318 there are a number of CD300lf polymorphisms in laboratory and wild mouse strains that
319 may affect CD300lf expression or conformation and thus may regulate susceptibility to
320 MNoV[49]. This raises the intriguing hypothesis of a molecular arms race between MNoV
321 and mice over evolutionary time which may have contributed to the relative avirulence of
322 MNoV in immunocompetent mice.

323 Finally, these data have several important implications for our understanding of
324 HNoV, the entry mechanisms of which remain to be defined. Given the structural similarity
325 between MNoV and HNoV as well as mouse and human CD300lf, we hypothesized that
326 human CD300lf might be a functional receptor for HNoV. However, via multiple
327 orthogonal approaches we demonstrated that human CD300lf is not a functional receptor
328 for several GI and GII HNoVs. This further raises the question as to the identity of the
329 HNoV receptor and whether or not it is structurally related to CD300lf. This remains an
330 important area of future investigation that would significantly enhance our understanding
331 of HNoV pathogenesis and facilitate novel prophylactic and therapeutic approaches.

332

333

Materials and Methods

Mouse strains

All mouse strains used in this experiment were from a C57BL/6J background (Jackson Laboratories, Bar Harbor, ME) and bred in-house. Generation of B6.CD300lf^{em1Cbwi}/J (*Cd300lf*$^{-/-}$) mice (Jackson Laboratories) and B6.129S(Cg)-Stat1^{tm1Div}/J (*Stat1*$^{-/-}$) (gift of H.W. Virgin) were previously described[15,50]. These mice were housed in a MNoV-free facility at Yale University School of Medicine. All experiments used littermate controls, were gender-balanced, and done at least two independent times. Mice were used for infections between 6-10 weeks of age. Genotyping of mice was done by real time PCR as described previously[15].

Ethics statement

The care and use of the animals were approved by and in agreement with the Yale Animal Resource Center and Institutional Animal Care and Use Committee (#2018-21098) according to standards in the *Animal Welfare Act*.

Viral stocks

MNoV^{CW3} (Gen bank accession EF014462.1), MNoV^{CR6} (accession JQ237823), and MNoV^{MNV3} (accession JQ658375.1) were generated from infectious molecular clones. MNoV^{CW3} is a plaque derived isolate of MNV-1[20]. MNoV^{F514I} was generated by site-directed mutagenesis of the parental MNoV^{CR6} plasmid. Plasmids containing infectious molecular clones were transfected into 293T cells (ATCC) to generate a P0 stock as previously described[15,20,51]. The P0 virus was passaged in BV2 cells (gift of H.W. Virgin)

to create a P1 stock that was used to inoculate BV2 cells at a 0.05 multiplicity of infection (MOI) for 36 hours to generate a working P2 stock. MNoV^{WU23} (accession EU004668), MNoV^{CR3} (accession EU004676.1), MNoV^{CR7} (accession EU004677), MNoV^{S99} (accession EF531291) were passaged RAW 264.7 cells (ATCC SC-6003) up to six times. RAW cell-derived virus was then expanded one time in BV2 cells as described above. Infected BV2 cell cultures were freeze/thawed, cell debris was pelleted at 1200g for 5 minutes (min), supernatant was filtered through a 0.22 μm filter and concentrated through a 100,000 MWCO Amicon Ultra filter. Virus stocks were aliquoted, tittered three independent times in duplicate, and stored at -80°C until use[15]. Sequencing of the MNoV capsid was performed by PCR amplification from viral cDNA using primers 5'-AACAACTTCACGGTCCAGTCGG3' and 5'-GCTTGAAAGAGTTGGCTTGGAGC-3' followed by Sanger sequencing by GENWIZ (South Plainfield, NJ). The P2 stock of MNoV^{F514I} was sequence confirmed by Sanger sequencing. MNoV VP1 alignment was performed with ESpript 3.0 software.

Cell line culture

BV2 cells, 293T cells, and HeLa cells (ATCC) were maintained in Dulbecco's modified eagle media (DMEM; Gibco, Gaithersburg, MD) supplemented with 10% fetal bovine serum (FBS; VWR, Radnor, PA), 1% pen/strep (Gibco), and 1% HEPES (Gibco). CD300lf-deficient BV2 cells (clone 1B6, BV2ΔCD300lf) were generated by CRISPR/Cas9[15]. BV2ΔCD300lf cells were complemented with transgenic CD300lf as described previously[15]. HIE cultures (Baylor College of Medicine) were maintained as previously described[8]. BL6/J bone marrow progenitors were isolated from CD300lf$^{-/-}$ or

CD300lf$^{+/-}$ mice as previously described[15,52]. Progenitors were differentiated into BMDMs by plating 10^6 cells into a 10 cm non-tissue culture treated dish with BMDM media (DMEM, 10% fetal bovine serum, 10% CMG14 conditioned media, 1 mM sodium pyruvate, 2 mM L-glutamine, 1% pen/strep) and incubated for seven days at 37°C and 5% CO_2[53]. BMDM differentiation was confirmed by flow cytometry staining for F4/80.

In vitro MNoV infections

BV2-WT and BV2ΔCD300lf cells (gift of H.W. Virgin) were seeded at 20,000 cells per well in 96-well plates and infected with diverse MNoV strains at a MOI of 5. After 48 hours, 25µL of CellTiter-Glo (Promega, Madison, WI) was added to each well and luminescence was detected on a Synergy luminometer (BioTek). Experiments were performed in duplicate in at least three independent experiments. BMDMs were infected for 24 hours with MNoV^{CW3} at a MOI 5 for flow cytometry experiments and a MOI 0.05 for plaque assays. Human enteroids were inoculated with HNoV GII.4 from stool filtrate as described previously[8]. Tranfected 293T cells were challenged with HNoV GII.6 from stool filtrate as described below. The HNoV GII.6 stool filtrate was determined to be infectious using BJAB cells as described previously[9].

In vitro HNoV infections in HIEs

Five-day differentiated jejunal HIE monolayers in 96-well plates were inoculated with HNoV GII.4_Sydney_2012 ($2.5x10^5$ genome copies/well) from stool filtrate as described previously[8]. Experiments were conducted in triplicate in three independent experiments. Serial dilutions of polyclonal antibody against huCD300LF (R&D Systems; AF2774) or

403 recombinant human CD300LF/LMIR3 Fc chimera protein (R&D Systems; 2774-LM-050)
404 samples were carried out in CMGF(-) medium containing 500 μM glycochenodeoxycholic
405 acid (GCDCA). An isotype control (Recombinant Human IgG1 Fc, CF; R&D Systems;
406 110-HG-100) and recombinant rotavirus NSP4 protein were used as controls
407 respectively. GII.4_Sydney_2012 ($2.5x10^5$ genome copies) were mixed with an equal
408 volume of media or dilutions of each serum or protein sample at 37ºC for 1 hr, and
409 inoculated onto jejunal HIE monolayers for another 1 hr at 37ºC in 5% CO_2. After
410 incubation, monolayers were washed twice with CMGF(-) media to remove unbound virus
411 and cultured in differentiation media with 500 μM GCDCA for the indicated time points.
412 RNA was extracted from each well using the KingFisher Flex Purification system and
413 MAgMAX-96 Viral RNA Isolation kit. RNA extracted at 1 hpi, was used as a baseline to
414 determine the amount of input virus that remained associated with cells after washing the
415 infected cultures to remove the unbound virus. Replication of virus was determined by
416 RNA levels quantified from samples extracted at 24 hpi.
417
418 **Mouse infections**
419 Mice were perorally (PO) inoculated with 25μL of 10^6 PFU MNoV diluted in D10 (DMEM
420 with 10% FBS). For intraperitoneal (IP) challenge, MNoV was diluted to either 10^7 or 10^6
421 PFU per 200μL in phosphate buffered saline (PBS) and injected into the left lower
422 quadrant of the peritoneal cavity with an insulin syringe. Fecal transmission assay was
423 performed by infecting *Cd300lf*$^{-/-}$ or *Cd300lf*$^{+/-}$ mice with 25μL PO of 10^6 PFU MNoV^{CR6}.
424 At seven dpi, a freshly isolated fecal pellet was homogenized in 100μL of PBS and 25μL
425 of the fecal slurry was administered PO to *Stat1*$^{-/-}$ mice. Seven days after fecal transfer,

fecal samples from the *Stat1*$^{-/-}$ recipient mice were tested for MNoV genomes via qPCR as described below.

Viral heat inactivation

Viral heat inactivation was performed by diluting MNoV^{CW3}, MNoV^{CR6}, and MNoV^{F514I} to 10^6 PFU per 50µL aliquots in D10 within PCR strip tubes. One aliquot of each virus tube was placed in a thermal cycler and heated at the following temperatures for 30 seconds: 37°, 47°, 52°, 55°, 58°, 61°, 62.5°, 64°, 67°, 70°, and 72°C. Samples were then immediately placed on ice, and 5µL of each sample was applied to 20,000 BV2 cells in 95µL in a 96-well plate. Cell viability was measured by CellTiter-Glo 48 hours post-infection as described above[15].

Virus quantification by plaque assay

BV2 cells were seeded in 6-well plates at 2 x10^6 cells/well. Tissue samples were weighed and homogenized with 1.0 mm silica beads (BioSpec, Bartlesville, OK) in 1 mL of D10 with 1% Pen/Strep, and 1% HEPES[38]. Tissue homogenates were serially diluted ten-fold. Media was aspirated off the BV2 cells and samples were inoculated to each well and gently rocked for 1 hour. Inoculum was removed and 2 mL of overlay media (MEM containing 1% methylcellulose, 10% FBS, 1% GlutaMAX (Gibco), 1% HEPES, and 1% pen/strep) was added to each well. Inoculated plates were incubated for 48 hours at 37°C and 5% CO_2 prior to plaque visualization with crystal violet (0.2% crystal violet in 20% ethanol) as described previously[37]. Plaque assay from cell culture was performed by

448 freeze/thawing infected samples at 0, 12, and 24 hpi followed by serial dilutions as
449 described above[15,37].
450
451 **Quantitative PCR**
452 MNoV genome copies in fecal pellets and tissues were determined as previously
453 described[15,54]. Briefly, viral RNA from fecal pellets was extracted using the Quick-RNA
454 Viral 96 Kits according to manufacturer's protocol (Zymo Research, Irvine, CA). Tissue
455 RNA extraction was performed using TRIzol (Life Technologies, Carlsbad, CA) and
456 purified using Direct-zol RNA MiniPrep Plus according to manufacturer's instructions
457 (Zymo Research). A two-step cDNA synthesis with 5µl RNA, random hexamer, and
458 ImProm-II Reverse Transcriptase (Promega) was performed[31]. Then, qPCR analysis was
459 performed in duplicate for each of the samples and standard curves generated using
460 MNoV specific oligonucleotides: Probe: 5' 6FAM-CGCTTTGGAACAATG-MGBNFQ 3';
461 Forward primer: 5' CACGCCACCGATCTGTTCTG 3'; Reverse primer: 5'
462 GCGCTGCGCCATCACTC 3'. The limit of detection was 10 MNoV genome copies/µL.
463 MNoV genome copies detected in tissues were normalized to the housekeeping gene β-
464 β-actin which was detected using murine β-actin oligonucleotides: Probe: 6-JOEN-
465 CACCAGTTC /ZEN/ GCCATGGATGACGA-IABkFQ 3'; Forward primer: 5' GCT CCT
466 TCG TTG CCG GTC CA 3'; Reverse primer: 5' TTG CAC ATG CCG GAG CCG TT 3'.
467 The actin limit of detection for qPCR was 100 copies/µL. Undetectable MNoV genomes
468 were set at 0.0001 relative to actin. For HNoV GII.6 qPCR, the primer pair NKP2F NKP2R
469 and probe RING2-TP were used as described previously[55]. For HNoV GII.4 qPCR, the
470 primer pair COG2R /QNIF2d and probe QNIFS were used[56]. A standard generated using

a 10-fold dilution series of a recombinant HuNoV RNA transcript was used to quantitate viral genome equivalents in RNA samples from GII.4 infected HIEs.

Flow cytometry

BMDMs were harvested after mock-inoculation or infection with MNoV. Cells were pelleted by centrifugation at 200 x g for 5 min and suspended in 250μL of Cytofix/Cytoperm (BD Biosciences) for 20 min at RT. Cells were washed twice with perm/wash buffer (PWB), suspended in staining buffer containing rabbit anti-NS1/2 antibody (1:1000; kind gift of Vernon Ward). The cells were incubated with antibody for 30 min at RT, pelleted and washed twice. The cells were suspended in staining buffer containing donkey anti-rabbit alexa fluor 647 (1:500, Life Technologies #A31573) and incubated for 30 min in the dark. The cells were pelleted and washed twice with PWB buffer. Cells were suspended in FACS buffer. Flow cytometry was performed on a MACSQuant Analyzer 10 (Miltenyi Biotec, Somerville, MA) and analyzed using FlowJo v10 (FlowJo LLC, Ashland, OR).

Mouse CD300 overexpression

HeLa cells were seeded at 400,000 cells per well in a 6-well plate and grown for 24 hours. Murine CD300lf and CD300ld (pcDNA3.4) were transiently transfected into HeLa cells with Trans-It LT1 (Mirus Bio, Madison, WI) according to manufacturer instructions[15]. $MNoV^{CW3}$, $MNoV^{CR6}$ and $MNoV^{F514I}$ were inoculated in transduced HeLa cells at a MOI of 5 and incubated for 24 hours at 37°C. Cells were harvested using Trypsin-EDTA and resuspended in FACS buffer (PBS containing 10% FBS and 2mM EDTA) and stained

494 with anti-CD300lf PE clone Tx70 (1:100; BioLegend, #132704) or anti-CD300ld PE clone
495 Tx69 (1:100, BioLegend, #139605). Cells were then stained intracellularly with guinea pig
496 anti-NS6/7 (kind gift from Kim Green) and goat anti-guinea pig Alexa Fluor 647 (1:500,
497 Life Technologies, #A21450). Cells were then washed twice with PWB and then
498 resuspended in FACS buffer.
499
500 **Neutralization Assay**
501 *Cd300lf*$^{-/-}$ or *Cd300lf*$^{+/-}$ mice were infected PO with 10^6 PFU MNoV^{CW3} and terminally bled
502 via cardiac puncture at 14 dpi. Whole blood was collected in an EDTA Microtainer tube
503 (BD) and pelleted at 5800 x g for 10 min. Plasma was removed and stored at 4°C until
504 use. BV2 cells were seeded at 20,000 cells in 50µL per well in a 96-cell plate and
505 incubated at 37°C. Sera were serially diluted in D10 with an initial dilution 1:9 and with
506 five subsequent three-fold dilutions. Then, 10^5 PFU of MNoV^{CW3} was added to each well
507 and mixtures were gently rocked for 30 min at room temperature (RT) and then added to
508 BV2 cells. After 48 hours, 25µL of CellTiter-Glo was added to each well and luminescence
509 was detected on a luminometer. Experiments were performed in duplicate with at least
510 three independent replicates.
511
512 **MNoV-specific ELISA**
513 In a 96-well MaxiSorp plate, 100µL of two-fold serially diluted IgG (starting at 12.5ng/mL)
514 and IgM (starting at 25ng/mL) was used as standard controls and MNoV^{CR6} was used to
515 coat the plate overnight at 4°C. The plate was then washed three times with 300µL wash
516 buffer (0.05% Tween-20 in PBS) and then blocked with 100µL of blocking solution (1%

BSA in PBS) for 1 hour at RT. After washing 3 times, 50μL of sample at appropriate dilutions in blocking solution was added to each well and incubated for 2 hours at RT. The plate was further washed three times and 50μL of anti-mouse IgG-HRP (A3673, Sigma-Aldrich) or anti-mouse IgM-HRP (A8786, Sigma-Aldrich) diluted in blocking solution was added to each well, then incubated for 2 hours at RT. Wells were washed three times, and then 40μL of ELISA TMB substrate solution (eBioscience, San Diego, CA) was added to each. Plates were incubated for 20 min, then 20μL of stop solution (2N H_2SO_4) added and OD determined at 450 nm and reference wavelength 570 nm.

ELISA for HuNoV VLPs binding to PGM

Pig gastric mucin (Sigma-Aldrich) was immobilized at 10 μg/ml in PBS on 96-well-plate at 4°C overnight. Wells were washed with PBS-0.05% Tween 20 (PBS-T) three times. After blocking with 5% non-fat milk at RT for 1 hour, plates were washed once with PBS-T. Fc-huCD300 proteins (10 μg/ml) were mixed with purified HuNoV VLPs at indicated concentrations and then added and incubated for 1 hour at RT. The wells were washed three times with PBS-T followed by addition of rabbit anti-VP1 sera diluted in PBS (1:2000). Wells were incubated at RT for 1 hour, followed by washing with PBS-T three times as described previously[44]. Secondary goat anti-rabbit-HRP diluted in PBS were added and incubated for 1 hour. After five washes, TMB substrate was added, and 2M H_2SO_4 was applied to stop the reaction. Absorbance at 450 nm was measured.

Statistical Analysis

All statistical analysis was performed in Prism GraphPad version 8 (San Diego, CA). Error bars represent the standard error of the mean unless otherwise indicated. Mann-Whitney tests were performed for all non-normally distributed data whereas normally distributed data was analyzed using Student's T-tests. All statistical tests were two-sided. Virus heat inactivation was analyzed using a one-way ANOVA. Survival experiments were analyzed by Kaplan-Meier survival curves. A p-value of <0.05 was considered significant (* p-value<0.05, ** p-value<0.01, *** p-value<0.001, **** p-value<0.0001).

Table 1.

Virus	Source mouse	Source tissue	Chronic infection	Systemic infection	Fecal Shedding	Accession	Ref
CW3	IFNαβγR$^{-/-}$	Brain	No	Yes	Limited	EF014462.1	14,20,58
CR6	B6 variant	Feces	Yes	No	Yes	EU004676.1	21
CR3	B6 variant	Feces	Yes	No	Yes	EU004676.1	21
CR7	B6 variant	Feces	Yes	No	Yes	EU004677	21
WU23	B6.OT1/ Rag1$^{-/-}$ /IFNγR$^{-/-}$	Feces	Unknown	Yes	Yes	EU004668	21
MNV-3	Pooled	MLN	Yes	No	Yes	JQ658375.1	59
S99	YFPH tg	Feces	Yes	No	Yes	EF531291	21,40

*B6, C57BL/6; B6 variant, unknown C57BL/6 genetically modified mouse; YFPH tg, Yellow fluorescent protein transgenic,

553 **Figure legends**

554 **Figure 1. CD300lf is necessary for MNoV^{CW3} infection *ex vivo* and *in vivo*.** (A-C)
555 BMDMs were generated from *Cd300lf*$^{-/-}$ and *Cd300lf*$^{+/-}$ littermate controls. (A) BMDMs
556 were challenged with MNoV^{CW3} (MOI= 0.05) and viral replication was measured by plaque
557 assay 24 hpi. (B) *Cd300lf*$^{+/-}$ and *Cd300lf*$^{-/-}$ BMDMs were challenged with MNoV^{CW3} (MOI=
558 5) and expression of the MNoV non-structural protein NS1/2 was measured by flow
559 cytometry. (C) Quanitifcation of NS1/2 expression. (D-E) *Cd300lf*$^{+/-}$ and *Cd300lf*$^{-/-}$
560 littermates were challenged with 10^6 PFU PO MNoV^{CW3}. 24 hpi, virus was measured by
561 both (D) plaque assay and (E) qPCR in the MLN, spleen, distal ileum, and proximal colon.
562 Data was analyzed by Mann-Whitney test. Shown are means ± SEM. NS, not significant;
563 *P<0.05; **P<0.01; ***P<0.001; L.O.D., limit of detection. Experiments in (A-C) where
564 performed at least two independent times each in triplicate. Data in (D-E) are pooled from
565 two independent experiments with at least three mice per group.

566
567 **Figure 2. CD300lf is necessary and sufficient for infection by diverse MNoV strains.**
568 (A) CD300lf WT and KO BV2 cells were infected with MNoV strains CW3, WU23, CR3,
569 CR7, MNV-3, and S99 at a MOI of 5. CD300lf KO BV2 cells were protected from virus-
570 induced cell death for all MNoV strains. (B) Mouse CD300ld (muCD300ld) and CD300lf
571 (muCD300lf) were overexpressed in human HeLa cells by transient transfection. Cells
572 were challenged with MNoV strains at a MOI of 5 for 24 hours and then infection was
573 quantified by MNoV NS6/7 expression by flow cytometry. (C-H) *Cd300lf*$^{+/-}$ or *Cd300lf*$^{-/-}$
574 mice were challenged with 10^6 PFU PO CW3, WU23, CR6, CR3, or CR7 for seven days.
575 MNoV was detectable in the (C) feces, (D) MLN, (E) spleen, (F) ileum, and (G) colon of
576 *Cd300lf*$^{+/-}$ but not *Cd300lf*$^{-/-}$ mice. (H) To test whether CR6 was shed in feces below the

limit of detection by qPCR, we gavaged *Stat*$^{-/-}$ mice with feces from *Cd300lf*$^{+/-}$ or *Cd300lf*$^{-/-}$ mice challenged with MNoV^{CR6} from (C). Fecal pellets from *Cd300lf*$^{-/-}$ mice, did not establish detectable infection in *Stat1*$^{-/-}$ mice. Data is pooled from two to four independent experiments. Data was analyzed by Mann-Whitney test. Shown are means ± SEM. NS, not significant; *P<0.05; **P<0.01; ***P<0.001; L.O.D., limit of detection.

Figure 3. CD300lf is required to generate humoral response after oral MNoV^{CW3} challenge. Sera was collected from *Cd300lf*$^{+/-}$ and *Cd300lf*$^{-/-}$ mice 14 days after challenge with 10^6 PFU PO MNoV^{CW3}. (A) The maximal protection (1:10 sera dilution) and (B) sera IC_{50} was measured by *in vitro* MNoV^{CW3} neutralization assay in BV2 cells. (C) *Cd300lf*$^{+/-}$ generated significantly increased anti-MNoV IgG (C) and IgM (D). Data is pooled from two independent experiments. Data was analyzed by Mann-Whitney test. Shown are means ± SEM. NS, not significant; *P<0.05; **P<0.01; ***P<0.001; ****P<0.0001. L.O.D., limit of detection.

Figure 4: CD300lf is essential for oral MNoV transmission in *Stat*$^{-/-}$ mice. (A) *Cd300lf*$^{+/+}$*Stat1*$^{-/-}$ (N=8) and *Cd300lf*$^{+/-}$*Stat1*$^{-/-}$ (N=4) mice challenged with 10^6 PFU PO MNoV^{CW3} succumbed to infection by 5 and 6 dpi, respectively. In contrast, all *Cd300lf*$^{-/-}$ *Stat1*$^{-/-}$ (N=10) mice survived for at least 21 dpi. (B-F) *Cd300lf*$^{+/+}$*Stat1*$^{-/-}$, *Cd300lf*$^{+/-}$*stat1*$^{-/-}$, and *Cd300lf*$^{-/-}$*Stat1*$^{-/-}$ mice were challenged with 10^6 PFU PO MNoV^{CR6}. All mice survived infection. Viral genomes were quantified in the (B) feces, (C) MLN, (D) spleen, (E) ileum, and (F) colon at seven dpi. Data is pooled from at least three independent experiments. Data was analyzed by Mann-Whitney test and Kaplan-Meier curves were generated for

601 survival experiments. Shown are means ± SEM. NS, not significant; *P<0.05; **P<0.01;
602 ***P<0.001; ****P<0.0001. L.O.D., limit of detection.
603
604 **Figure 5. CD300lf is essential for pathogenesis of parenterally transmitted MNoV in**
605 **STAT1 deficient mice**. (A) Mice were challenged with 10^7 PFU IP MNoV^{CW3}. *Cd300lf*$^{-/-}$
606 *Stat1*$^{-/-}$ mice (N=9 mice) survived infection in contrast to *Cd300lf*$^{+/+}$*Stat1*$^{-/-}$ (N=15 mice)
607 and *Cd300lf*$^{+/-}$*Stat1*$^{-/-}$ (N=9 mice) littermates. (B) Mice were challenged with 10^7 PFU IP
608 MNoV^{CR6}. *Cd300lf*$^{-/-}$*Stat1*$^{-/-}$ mice (N=6 mice) survived infection in contrast to
609 *Cd300lf*$^{+/+}$*Stat1*$^{-/-}$ (N=9 mice) and *Cd300lf*$^{+/-}$*Stat1*$^{-/-}$ (N=3 mice) littermates. (C) MNoV
610 genomes were quantified from the MLN, spleen, ileum, and colon of *Cd300lf*$^{-/-}$*Stat1*$^{-/-}$ mice
611 seven days post-challenge with 10^7 PFU IP MNoV^{CR6}. Data was analyzed by Kaplan-
612 Meier curve for survival experiments. Data is pooled from at least three independent
613 experiments with 1-5 mice per group. *P<0.05; **P<0.01; ***P<0.001; ****P<0.0001.
614 L.O.D., limit of detection.
615
616 **Figure 6. Emergence of MNoV^{F514I} variant after high dose intraperitoneal challenge**
617 **in *Cd300lf*$^{-/-}$*Stat1*$^{-/-}$ mice.** Sanger sequencing revealed a single amino acid mutation in
618 the P1 domain of MNoV^{CR6} after IP challenge with 10^7 PFU MNoV^{CR6} in *Cd300lf*$^{-/-}$*Stat1*$^{-/-}$
619 mice. An infectious molecular clone of MNoV^{F514I} was generated**.** (A) MNoV^{F514I} mediated
620 cell death of BV2 cells is CD300lf dependent. (B) HeLa cells transiently expressing murine
621 CD300ld (muCD300ld) or murine CD300lf (muCD300lf) where challenged with MNoV^{CR6}
622 or MNoV^{F514I} (MOI of 5). MNoV infection was determined by expression of MNoV NS6/7
623 by flow cytometry. MNoV^{F514I} and MNoV^{CR6} similarly utilize muCD300ld and muCD300lf

when overexpressed. (C) $MNoV^{F514I}$ and $MNoV^{CR6}$ have similar thermal stability which differs from $MNoV^{CW3}$. (D) *Cd300lf*$^{+/-}$ and *Cd300lf*$^{-/-}$ mice were challenged with 10^6 PFU PO $MNoV^{F514I}$. Viral genomes were quantified in the (D) MLN, (E) spleen, (F) ileum, (G) colon and (H) feces at seven dpi. $MNoV^{F514I}$ infection was detected in *Cd300lf*$^{+/-}$ mice but not *Cd300lf*$^{-/-}$ mice. Data was analyzed by Mann-Whitney tests. Shown are means ± SEM. NS, not significant; *P<0.05; **P<0.01; ***P<0.001; L.O.D., limit of detection.

Figure 7. Human CD300lf is not a HNoV entry factor. (A) Human CD300lf and human CD300ld Fc-fusion proteins do not prevent binding of HNoV virus-like particles (VLPs) to pig gastric mucin for GI.1 Norwalk, GI.3 Desert Shield Virus, GII.4.1997, and GII.4.2012. (B) Polyclonal antibody against human CD300lf does not prevent HNoV GII.4 replication in HIEs relative to an IgG1 control. (C) Pre-incubating HNoV GII.4 with a human CD300lf Fc-fusion protein does not prevent HNoV replication in HIEs relative to a control protein (RV NSP4). Data in (A) is representative of at least two independent replicates each performed in duplicate. Data in (B and C) is pooled from three independent experiments with each condition and time point performed in triplicate wells of HIE cultures. Shown are means ± standard deviation.

Figure S1. Tree and VP1 alignment showing CD300 interacting sites. VP1 is the major structural protein of MNoV and is comprised of a shell and protruding domain. The complete VP1 sequence of MNoV strains CW3, CR6, CR3, CR7, WU23, MNV3, and S99 were aligned. The VP1 shell domain comprises the core of the virion and is sufficient for virion assembly. The protruding domain mediates binding to CD300lf and bile salts and

647 is comprised of discontinuous P1 and P2 subdomains. The CD300lf and secondary bile
648 acid (GCDCA) binding sites are highlighted as is the F514I mutation which emerged
649 during infection of *Cd300lf*$^{-/-}$*Stat1*$^{-/-}$ mice[13]. Secondary structures labeled as alpha-helices
650 (α), 3_{10}-helices (η), and beta-strands (β). The number following the annotation is the
651 numerical order of that secondary structure. Helices are displayed as squiggles and
652 strands are represented by a forward moving arrow under the annotation. TT = strict β-
653 turns and TTT = strict α turns.
654

655 **Acknowledgements**: We would like to acknowledge Herbert Virgin, Darren
656 Kreamalmeyer, Stephanie Karst, Adam Huys, and Joan Stayos for helpful discussions,
657 generously providing reagents, and technical support. This work was supported by NIH
658 grants K08 AI128043 (CBW), K22 AI151446 (MTB), R01 AI127552 (MTB), R01 AI139314
659 (MTB), T32 GM007067 (FCW), K99 DK116666 (RCO), and Wellcome Trust
660 [203268/z/16/z] (RSB). CBW was also supported by a Burroughs Wellcome Fund Career
661 Award for Medical Scientists. MTB was also supported by the Pew Biomedical Scholars
662 Program. EAK was supported by NSF Graduate Research Fellowship DGE-1745038.
663 The funders had no role in study design, data collection and analysis, decision to publish,
664 or preparation of the manuscript. CBW and RCO are inventors on a patent application
665 submitted by Washington University entitled “Receptor for norovirus and uses thereof”
666 (U.S. Provisional Application 62/301,965). All relevant data is included in the manuscript.
667

668 **Author contributions:** VRG, EAK, FCW, EH, JW, KE, MSS, RBF, LLH, AH, and CBW
669 performed experiments. AOK, CEW, LCL, and RSB provided critical reagents. VRG,

670 SMK, MKE, RCO, MTB, and CBW designed the project. VRG, EAK, FCW, EH, JW, KE,

671 AH, SMK, MKE, RCO, MTB, and CBW analyzed data. VRG, MTB, CBW wrote the paper.

672 All authors read and edited the manuscript.

673

References

1. Graziano VR, Wei J, Wilen CB. Norovirus Attachment and Entry. *Viruses.* 2019;11(6).
2. Lopman BA, Steele D, Kirkwood CD, Parashar UD. The Vast and Varied Global Burden of Norovirus: Prospects for Prevention and Control. *PLoS Med.* 2016;13(4):e1001999.
3. Ahmed SM, Hall AJ, Robinson AE, et al. Global prevalence of norovirus in cases of gastroenteritis: a systematic review and meta-analysis. *Lancet Infect Dis.* 2014;14(8):725-730.
4. Ahmed SM, Lopman BA, Levy K. A systematic review and meta-analysis of the global seasonality of norovirus. *PLoS One.* 2013;8(10):e75922.
5. Marsh M, Helenius A. Virus entry: open sesame. *Cell.* 2006;124(4):729-740.
6. Estes MK, Ettayebi K, Tenge VR, et al. Human Norovirus Cultivation in Nontransformed Stem Cell-Derived Human Intestinal Enteroid Cultures: Success and Challenges. *Viruses.* 2019;11(7).
7. Kilic T, Koromyslova A, Hansman GS. Structural Basis for Human Norovirus Capsid Binding to Bile Acids. *J Virol.* 2019;93(2).
8. Ettayebi K, Crawford SE, Murakami K, et al. Replication of human noroviruses in stem cell-derived human enteroids. *Science.* 2016.
9. Jones MK, Watanabe M, Zhu S, et al. Enteric bacteria promote human and mouse norovirus infection of B cells. *Science.* 2014;346(6210):755-759.
10. Karst SM, Wobus CE, Goodfellow IG, Green KY, Virgin HW. Advances in norovirus biology. *Cell Host Microbe.* 2014;15(6):668-680.

11. Walker FC, Baldridge MT. Interactions between noroviruses, the host, and the microbiota. *Curr Opin Virol.* 2019;37:1-9.

12. Sherman MB, Williams AN, Smith HQ, et al. Bile salts alter the mouse norovirus capsid conformation; possible implications for cell attachment and immune evasion. *J Virol.* 2019.

13. Nelson CA, Wilen CB, Dai YN, et al. Structural basis for murine norovirus engagement of bile acids and the CD300lf receptor. *Proc Natl Acad Sci U S A.* 2018;115(39):E9201-E9210.

14. Karst SM, Wobus CE, Lay M, Davidson J, Virgin HW. STAT1-dependent innate immunity to a Norwalk-like virus. *Science.* 2003;299(5612):1575-1578.

15. Orchard RC, Wilen CB, Doench JG, et al. Discovery of a proteinaceous cellular receptor for a norovirus. *Science.* 2016;353(6302):933-936.

16. Haga K, Fujimoto A, Takai-Todaka R, et al. Functional receptor molecules CD300lf and CD300ld within the CD300 family enable murine noroviruses to infect cells. *Proc Natl Acad Sci U S A.* 2016;113(41):E6248-E6255.

17. Prasad BV, Rothnagel R, Jiang X, Estes MK. Three-dimensional structure of baculovirus-expressed Norwalk virus capsids. *J Virol.* 1994;68(8):5117-5125.

18. Jiang X, Wang M, Graham DY, Estes MK. Expression, self-assembly, and antigenicity of the Norwalk virus capsid protein. *J Virol.* 1992;66(11):6527-6532.

19. Kilic T, Koromyslova A, Malak V, Hansman GS. Atomic Structure of the Murine Norovirus Protruding Domain and Soluble CD300lf Receptor Complex. *J Virol.* 2018;92(11).

719 20. Strong DW, Thackray LB, Smith TJ, Virgin HW. Protruding domain of capsid
720 protein is necessary and sufficient to determine murine norovirus replication and
721 pathogenesis in vivo. *J Virol.* 2012;86(6):2950-2958.
722 21. Thackray LB, Wobus CE, Chachu KA, et al. Murine noroviruses comprising a
723 single genogroup exhibit biological diversity despite limited sequence divergence.
724 *J Virol.* 2007;81(19):10460-10473.
725 22. Ward JM, Wobus CE, Thackray LB, et al. Pathology of immunodeficient mice
726 with naturally occurring murine norovirus infection. *Toxicol Pathol.*
727 2006;34(6):708-715.
728 23. Nice TJ, Strong DW, McCune BT, Pohl CS, Virgin HW. A single-amino-acid
729 change in murine norovirus NS1/2 is sufficient for colonic tropism and
730 persistence. *J Virol.* 2013;87(1):327-334.
731 24. Van Winkle JA, Robinson BA, Peters AM, et al. Persistence of Systemic Murine
732 Norovirus Is Maintained by Inflammatory Recruitment of Susceptible Myeloid
733 Cells. *Cell Host Microbe.* 2018;24(5):665-676.e664.
734 25. Borrego F. The CD300 molecules: an emerging family of regulators of the
735 immune system. *Blood.* 2013;121(11):1951-1960.
736 26. Voss OH, Tian L, Murakami Y, Coligan JE, Krzewski K. Emerging role of CD300
737 receptors in regulating myeloid cell efferocytosis. *Mol Cell Oncol.*
738 2015;2(4):e964625.
739 27. Tian L, Choi SC, Murakami Y, et al. p85α recruitment by the CD300f
740 phosphatidylserine receptor mediates apoptotic cell clearance required for
741 autoimmunity suppression. *Nat Commun.* 2014;5:3146.

28. Xi H, Katschke KJ, Helmy KY, et al. Negative regulation of autoimmune demyelination by the inhibitory receptor CLM-1. *J Exp Med.* 2010;207(1):7-16.

29. Rozenberg P, Reichman H, Moshkovits I, Munitz A. CD300 family receptors regulate eosinophil survival, chemotaxis, and effector functions. *J Leukoc Biol.* 2018;104(1):21-29.

30. Moshkovits I, Reichman H, Karo-Atar D, et al. A key requirement for CD300f in innate immune responses of eosinophils in colitis. *Mucosal Immunol.* 2017;10(1):172-183.

31. Wilen CB, Lee S, Hsieh LL, et al. Tropism for tuft cells determines immune promotion of norovirus pathogenesis. *Science.* 2018;360(6385):204-208.

32. Glass RI, Parashar UD, Estes MK. Norovirus gastroenteritis. *N Engl J Med.* 2009;361(18):1776-1785.

33. Parrino TA, Schreiber DS, Trier JS, Kapikian AZ, Blacklow NR. Clinical immunity in acute gastroenteritis caused by Norwalk agent. *N Engl J Med.* 1977;297(2):86-89.

34. Kapikian AZ, Wyatt RG, Dolin R, Thornhill TS, Kalica AR, Chanock RM. Visualization by immune electron microscopy of a 27-nm particle associated with acute infectious nonbacterial gastroenteritis. *J Virol.* 1972;10(5):1075-1081.

35. Karst SM, Tibbetts SA. Recent advances in understanding norovirus pathogenesis. *J Med Virol.* 2016;88(11):1837-1843.

36. Karst SM, Wobus CE. A working model of how noroviruses infect the intestine. *PLoS Pathog.* 2015;11(2):e1004626.

764 37. Wobus CE, Karst SM, Thackray LB, et al. Replication of Norovirus in cell culture
765 reveals a tropism for dendritic cells and macrophages. *PLoS Biol.*
766 2004;2(12):e432.
767 38. Grau KR, Roth AN, Zhu S, et al. The major targets of acute norovirus infection
768 are immune cells in the gut-associated lymphoid tissue. *Nat Microbiol.*
769 2017;2(12):1586-1591.
770 39. Kolawole AO, Smith HQ, Svoboda SA, et al. Norovirus Escape from Broadly
771 Neutralizing Antibodies Is Limited to Allostery-Like Mechanisms. *mSphere.*
772 2017;2(5).
773 40. Müller B, Klemm U, Mas Marques A, Schreier E. Genetic diversity and
774 recombination of murine noroviruses in immunocompromised mice. *Arch Virol.*
775 2007;152(9):1709-1719.
776 41. Niendorf S, Klemm U, Mas Marques A, Bock CT, Höhne M. Infection with the
777 Persistent Murine Norovirus Strain MNV-S99 Suppresses IFN-Beta Release and
778 Activation of Stat1 In Vitro. *PLoS One.* 2016;11(6):e0156898.
779 42. Snowden JS, Hurdiss DL, Adeyemi OO, Ranson NA, Herod MR, Stonehouse NJ.
780 High-Resolution Cryo-EM Reveals Dynamics in the Murine Norovirus Capsid.
781 *bioRxiv.* 2019:693143.
782 43. Harrington PR, Vinjé J, Moe CL, Baric RS. Norovirus capture with histo-blood
783 group antigens reveals novel virus-ligand interactions. *J Virol.* 2004;78(6):3035-
784 3045.
785 44. Harrington PR, Lindesmith L, Yount B, Moe CL, Baric RS. Binding of Norwalk
786 virus-like particles to ABH histo-blood group antigens is blocked by antisera from

787 infected human volunteers or experimentally vaccinated mice. *J Virol.*
788 2002;76(23):12335-12343.
789 45. Jiang C, Parrish NF, Wilen CB, et al. Primary infection by a human
790 immunodeficiency virus with atypical coreceptor tropism. *J Virol.*
791 2011;85(20):10669-10681.
792 46. Wilen CB, Parrish NF, Pfaff JM, et al. Phenotypic and immunologic comparison
793 of clade B transmitted/founder and chronic HIV-1 envelope glycoproteins. *J Virol.*
794 2011;85(17):8514-8527.
795 47. Haber AL, Biton M, Rogel N, et al. A single-cell survey of the small intestinal
796 epithelium. *Nature.* 2017;551(7680):333-339.
797 48. Lindesmith LC, Donaldson EF, Beltramello M, et al. Particle conformation
798 regulates antibody access to a conserved GII.4 norovirus blockade epitope. *J*
799 *Virol.* 2014;88(16):8826-8842.
800 49. Clark GJ, Ju X, Tate C, Hart DN. The CD300 family of molecules are
801 evolutionarily significant regulators of leukocyte functions. *Trends Immunol.*
802 2009;30(5):209-217.
803 50. Durbin JE, Hackenmiller R, Simon MC, Levy DE. Targeted disruption of the
804 mouse Stat1 gene results in compromised innate immunity to viral disease. *Cell.*
805 1996;84(3):443-450.
806 51. Arias A, Bailey D, Chaudhry Y, Goodfellow I. Development of a reverse-genetics
807 system for murine norovirus 3: long-term persistence occurs in the caecum and
808 colon. *J Gen Virol.* 2012;93(Pt 7):1432-1441.

52. Wang GG, Calvo KR, Pasillas MP, Sykes DB, Häcker H, Kamps MP. Quantitative production of macrophages or neutrophils ex vivo using conditional Hoxb8. *Nat Methods.* 2006;3(4):287-293.

53. Takeshita S, Kaji K, Kudo A. Identification and characterization of the new osteoclast progenitor with macrophage phenotypes being able to differentiate into mature osteoclasts. *J Bone Miner Res.* 2000;15(8):1477-1488.

54. Baert L, Wobus CE, Van Coillie E, Thackray LB, Debevere J, Uyttendaele M. Detection of murine norovirus 1 by using plaque assay, transfection assay, and real-time reverse transcription-PCR before and after heat exposure. *Appl Environ Microbiol.* 2008;74(2):543-546.

55. Jones MK, Grau KR, Costantini V, et al. Human norovirus culture in B cells. *Nat Protoc.* 2015;10(12):1939-1947.

56. Loisy F, Atmar RL, Guillon P, Le Cann P, Pommepuy M, Le Guyader FS. Real-time RT-PCR for norovirus screening in shellfish. *J Virol Methods.* 2005;123(1):1-7.

57. Martínez-Barriocanal A, Comas-Casellas E, Schwartz S, Martín M, Sayós J. CD300 heterocomplexes, a new and family-restricted mechanism for myeloid cell signaling regulation. *J Biol Chem.* 2010;285(53):41781-41794.

58. Mumphrey SM, Changotra H, Moore TN, et al. Murine norovirus 1 infection is associated with histopathological changes in immunocompetent hosts, but clinical disease is prevented by STAT1-dependent interferon responses. *J Virol.* 2007;81(7):3251-3263.

831 59. Hsu CC, Riley LK, Wills HM, Livingston RS. Persistent infection with and
832 serologic cross-reactivity of three novel murine noroviruses. *Comp Med.*
833 2006;56(4):247-251.

834

Figure 1

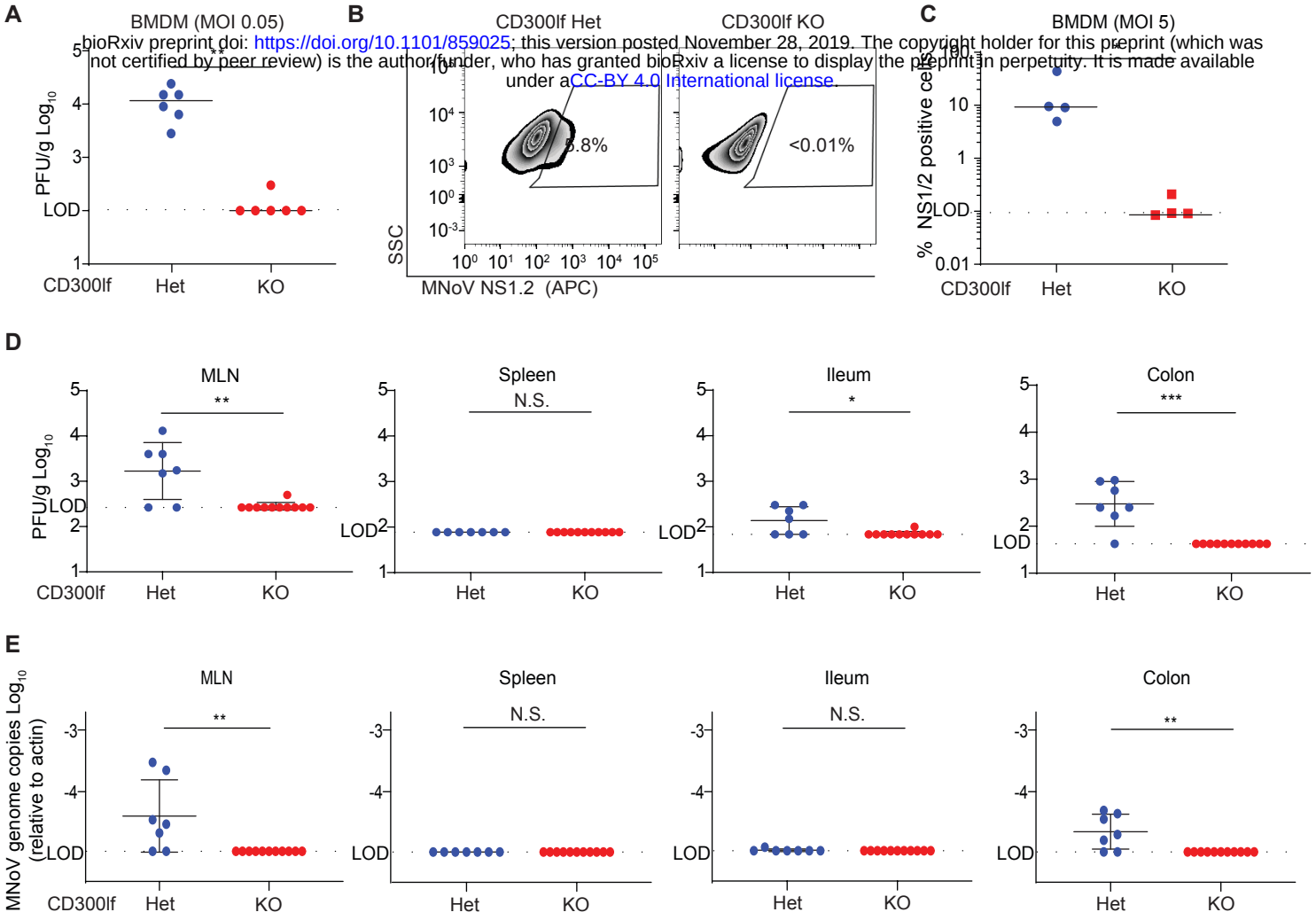

Figure 1. CD300lf is necessary for MNoVCW3 infection ex vivo and in vivo. (A-C) BMDMs were generated from Cd300lf-/- and Cd300lf+/- littermate controls. (A) BMDMs were challenged with MNoVCW3 (MOI= 0.05) and viral replication was measured by plaque assay 24 hpi. (B) Cd300lf+/- and Cd300lf-/- BMDMs were challenged with MNoVCW3 (MOI= 5) and expression of the MNoV non-structural protein NS1/2 was measured by flow cytometry. (C) Quanitifcation of NS1/2 expression. (D-E) Cd300lf+/- and Cd300lf-/- littermates were challenged with 106 PFU PO MNoVCW3. 24 hpi, virus was measured by both (D) plaque assay and (E) qPCR in the MLN, spleen, distal ileum, and proximal colon. Data was analyzed by Mann-Whitney test. Shown are means ± SEM. NS, not significant; *P<0.05; **P<0.01; ***P<0.001; L.O.D., limit of detection. Experiments in (A-C) where performed at least two independent times each in triplicate. Data in (D-E) are pooled from two independent experiments with at least three mice per group.

Figure 2

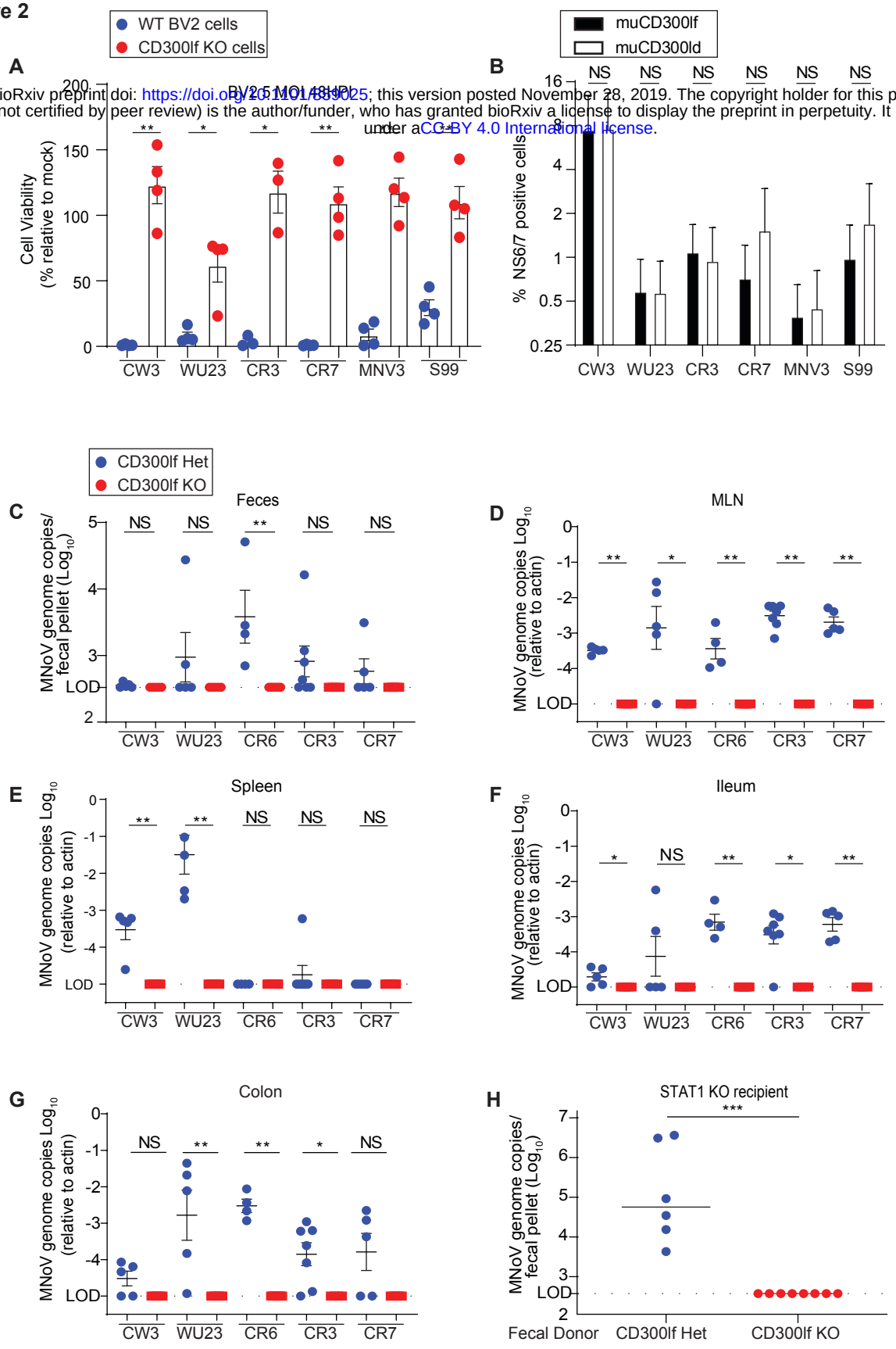

Figure 2. CD300lf is necessary and sufficient for infection by diverse MNoV strains. (A) CD300lf WT and KO BV2 cells were infected with MNoV strains CW3, WU23, CR3, CR7, MNV-3, and S99 at a MOI of 5. CD300lf KO BV2 cells were protected from virus-induced cell death for all MNoV strains. (B) Mouse CD300ld (muCD300ld) and CD300lf (muCD300lf) were overexpressed in human HeLa cells by transient transfection. Cells were challenged with MNoV strains at a MOI of 5 for 24 hours and then infection was quantified by MNoV NS6/7 expression by flow cytometry. (C-H) Cd300lf+/- or Cd300lf-/- mice were challenged with 106 PFU PO CW3, WU23, CR6, CR3, or CR7 for seven days. MNoV was detectable in the (C) feces, (D) MLN, (E) spleen, (F) ileum, and (G) colon of Cd300lf+/- but not Cd300lf-/- mice. (H) To test whether CR6 was shed in feces below the limit of detection by qPCR, we gavaged Stat-/- mice with feces from Cd300lf+/- or Cd300lf-/- mice challenged with MNoVCR6 from (C). Fecal pellets from Cd300lf-/- mice, did not establish detectable infection in Stat1-/- mice. Data is pooled from two to four independent experiments. Data was analyzed by Mann-Whitney test. Shown are means ± SEM. NS, not significant; *P<0.05; **P<0.01; ***P<0.001; L.O.D., limit of detection.

Figure 3

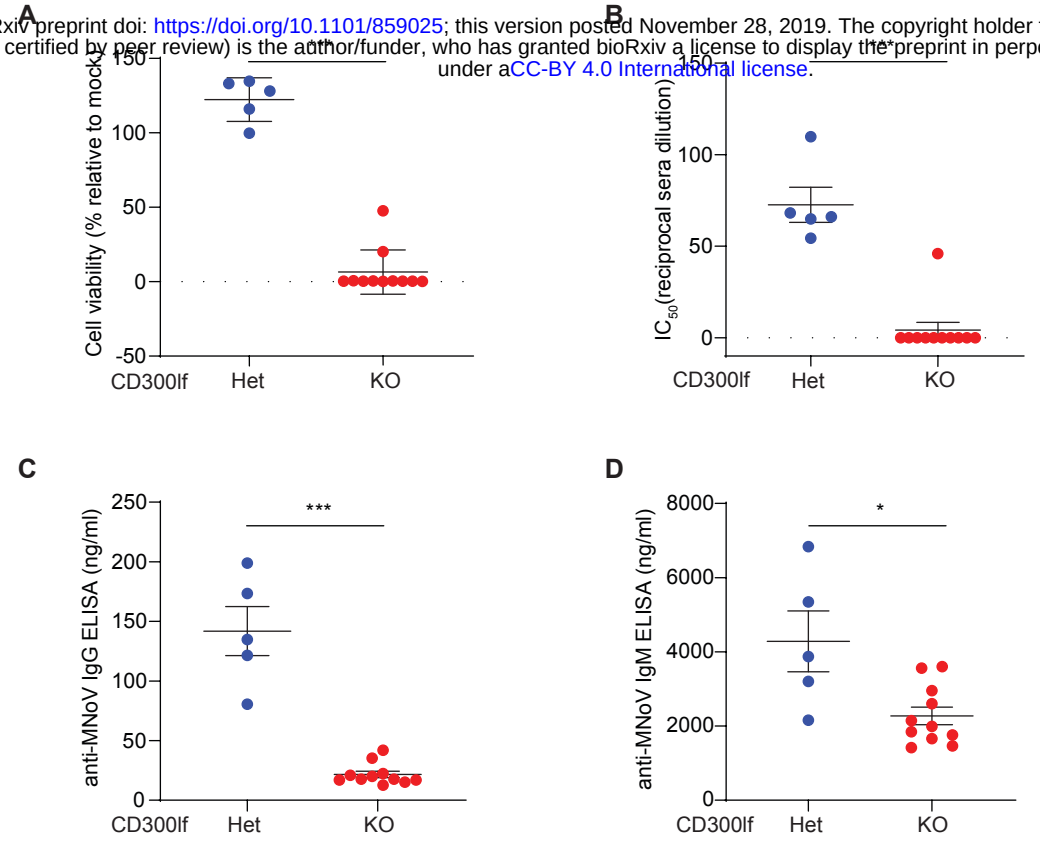

Figure 3. CD300lf is required to generate humoral response after oral MNoVCW3 challenge. Sera was collected from Cd300lf+/- and Cd300lf-/- mice 14 days after challenge with 106 PFU PO MNoVCW3. (A) The maximal protection (1:10 sera dilution) and (B) sera IC50 was measured by in vitro MNoVCW3 neutralization assay in BV2 cells. (C) Cd300lf+/- generated significantly increased anti-MNoV IgG (C) and IgM (D). Data is pooled from two independent experiments. Data was analyzed by Mann-Whitney test. Shown are means ± SEM. NS, not significant; *P<0.05; **P<0.01; ***P<0.001; ****P<0.0001. L.O.D., limit of detection.

Figure 4

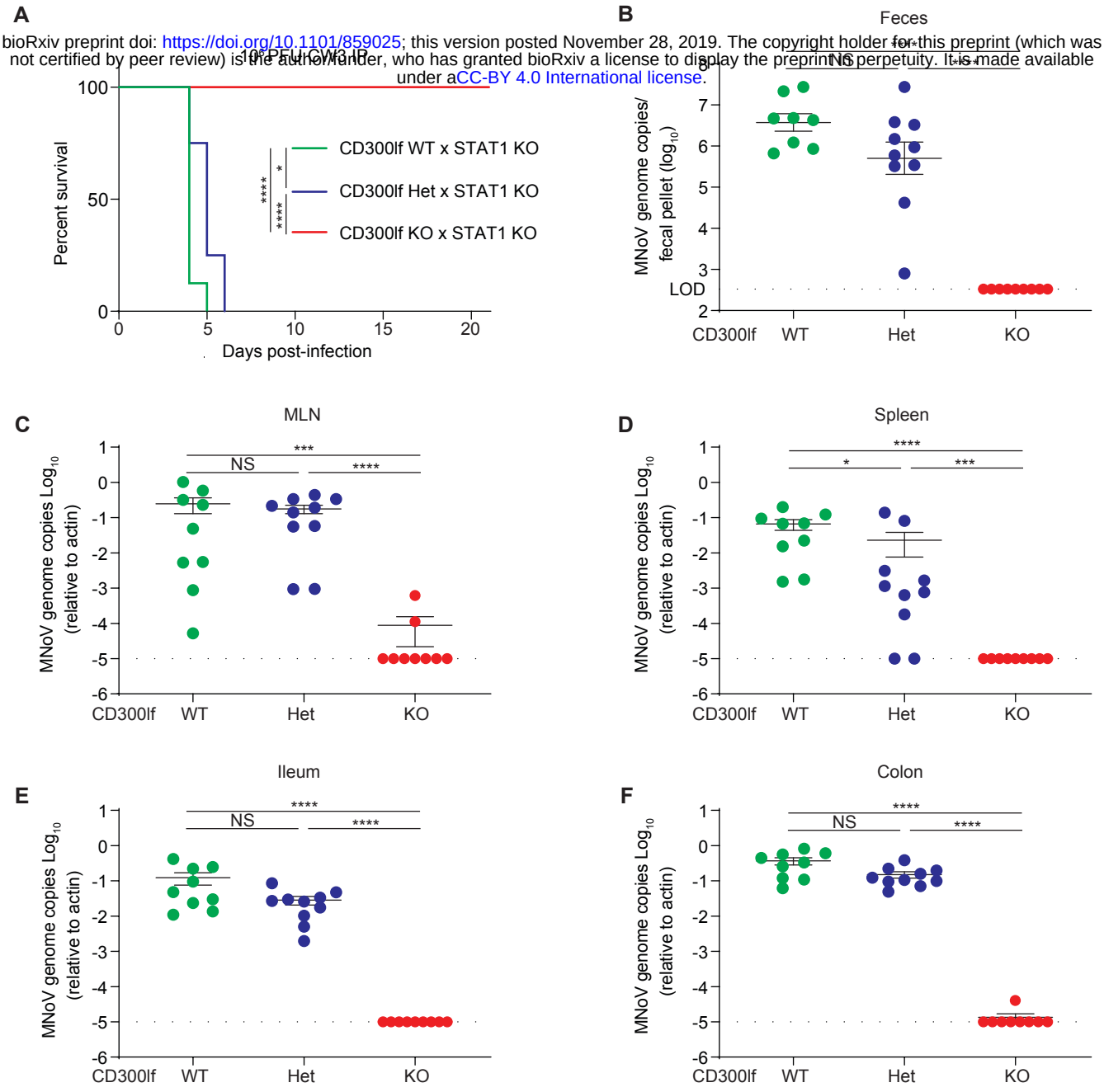

Figure 4: CD300lf is essential for oral MNoV transmission in Stat-/- mice.
(A) Cd300lf+/+Stat1-/- (N=8) and Cd300lf+/-Stat1-/- (N=4) mice challenged with 106 PFU PO MNoVCW3 succumbed to infection by 5 and 6 dpi, respectively. In contrast, all Cd300lf-/-Stat1-/- (N=10) mice survived for at least 21 dpi. (B-F) Cd300lf+/+Stat1-/-, Cd300lf+/-stat1-/-, and Cd300lf-/-Stat1-/- mice were challenged with 106 PFU PO MNoVCR6. All mice survived infection. Viral genomes were quantified in the (B) feces, (C) MLN, (D) spleen, (E) ileum, and (F) colon at seven dpi. Data is pooled from at least three independent experiments. Data was analyzed by Mann-Whitney test and Kaplan-Meier curves were generated for survival experiments. Shown are means ± SEM. NS, not significant; *P<0.05; **P<0.01; ***P<0.001; ****P<0.0001. L.O.D., limit of detection.

Figure 5

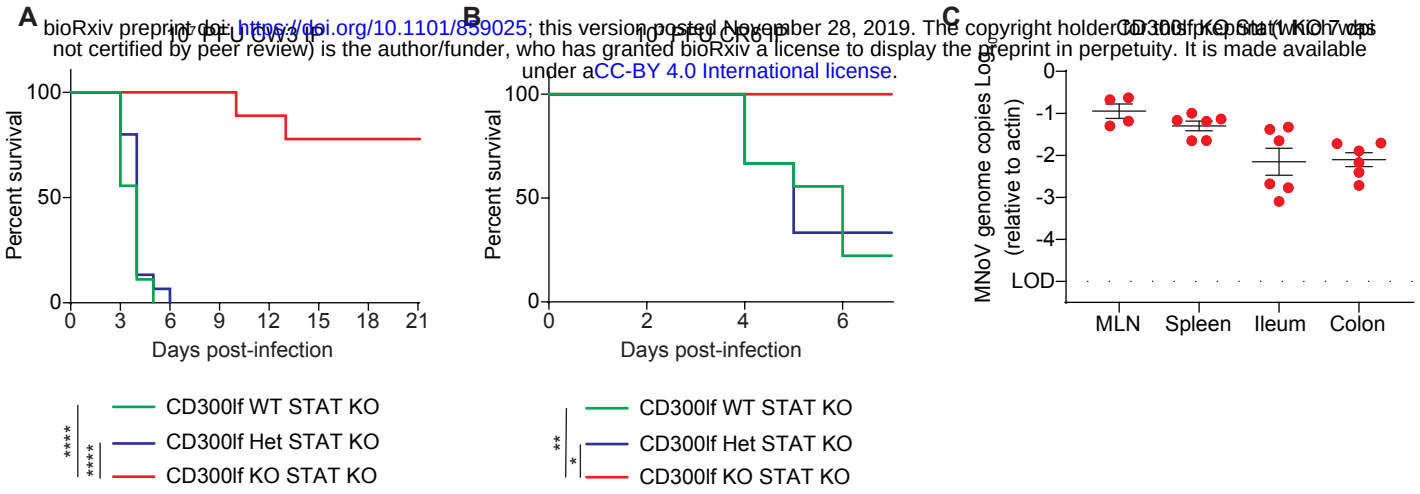

Figure 5. CD300lf is essential for pathogenesis of parenterally transmitted MNoV in STAT1 deficient mice. (A) Mice were challenged with 107 PFU IP MNoVCW3. Cd300lf-/-Stat1-/- mice (N=9 mice) survived infection in contrast to Cd300lf+/+Stat1-/- (N=15 mice) and Cd300lf+/-Stat1-/- (N=9 mice) littermates. (B) Mice were challenged with 107 PFU IP MNoVCR6. Cd300lf-/-Stat1-/- mice (N=6 mice) survived infection in contrast to Cd300lf+/+Stat1-/- (N=9 mice) and Cd300lf+/-Stat1-/- (N=3 mice) littermates. (C) MNoV genomes were quantified from the MLN, spleen, ileum, and colon of Cd300lf-/-Stat1-/- mice seven days post-challenge with 107 PFU IP MNoVCR6. Data was analyzed by Kaplan-Meier curve for survival experiments. Data is pooled from at least three independent experiments with 1-5 mice per group. *P<0.05; **P<0.01; ***P<0.001; ****P<0.0001. L.O.D., limit of detection.

Figure 6

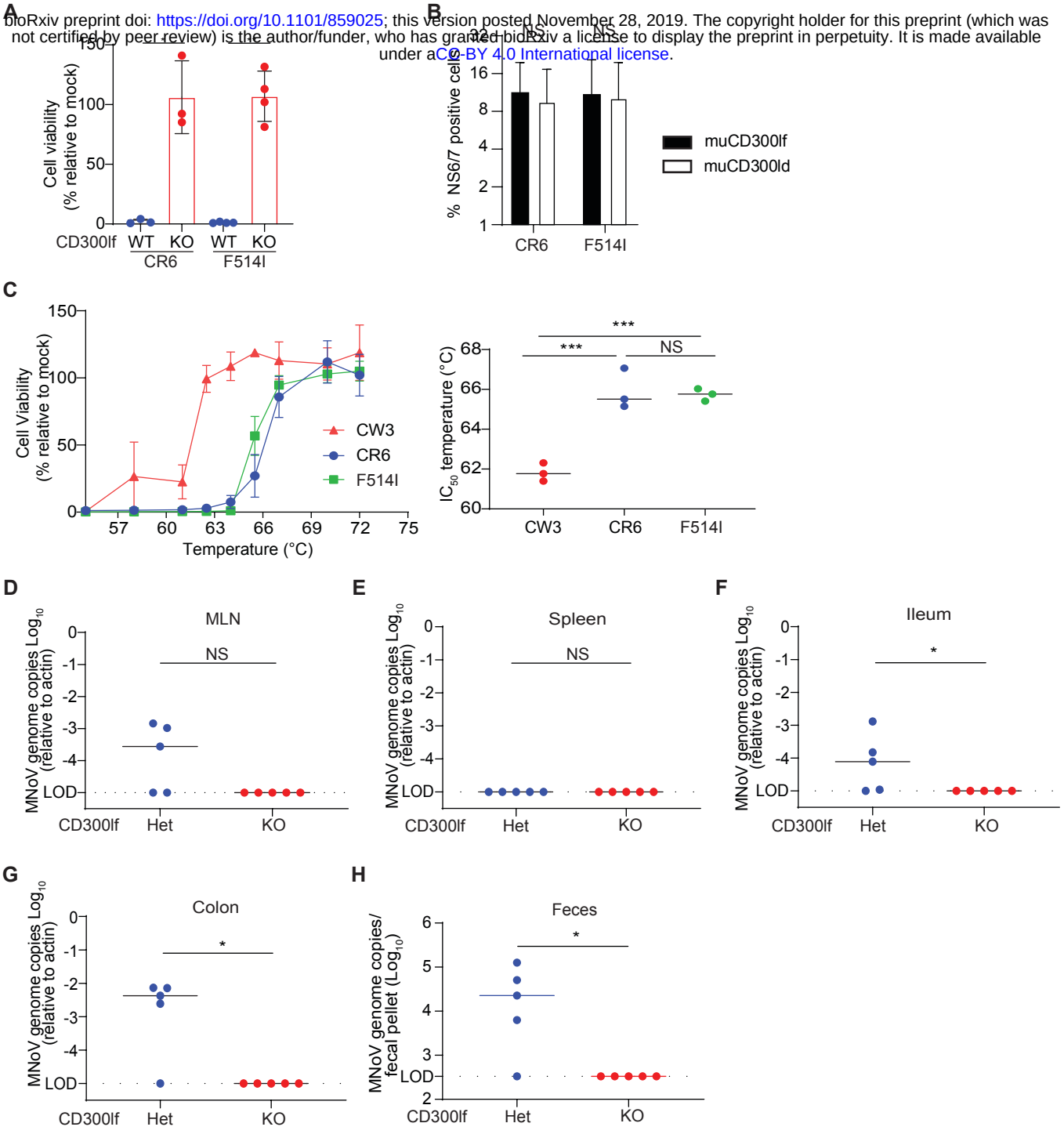

Figure 6. Emergence of MNoVF514I variant after high dose intraperitoneal challenge in Cd300lf-/-Stat1-/- mice. Sanger sequencing revealed a single amino acid mutation in the P1 domain of MNoVCR6 after IP challenge with 107 PFU MNoVCR6 in Cd300lf-/-Stat1-/- mice. An infectious molecular clone of MNoVF514I was generated. (A) MNoVF514I mediated cell death of BV2 cells is CD300lf dependent. (B) HeLa cells transiently expressing murine CD300ld (muCD300ld) or murine CD300lf (muCD300lf) where challenged with MNoVCR6 or MNoVF514I (MOI of 5). MNoV infection was determined by expression of MNoV NS6/7 by flow cytometry. MNoVF514I and MNoVCR6 similarly utilize muCD300ld and muCD300lf when overexpressed. (C) MNoVF514I and MNoVCR6 have similar thermal stability which differs from MNoVCW3. (D) Cd300lf+/- and Cd300lf-/- mice were challenged with 106 PFU PO MNoVF514I. Viral genomes were quantified in the (D) MLN, (E) spleen, (F) ileum, (G) colon and (H) feces at seven dpi. MNoVF514I infection was detected in Cd300lf+/- mice but not Cd300lf-/- mice. Data was analyzed by Mann-Whitney tests. Shown are means ± SEM. NS, not significant; *P<0.05; **P<0.01; ***P<0.001; L.O.D., limit of detection.

Figure 7

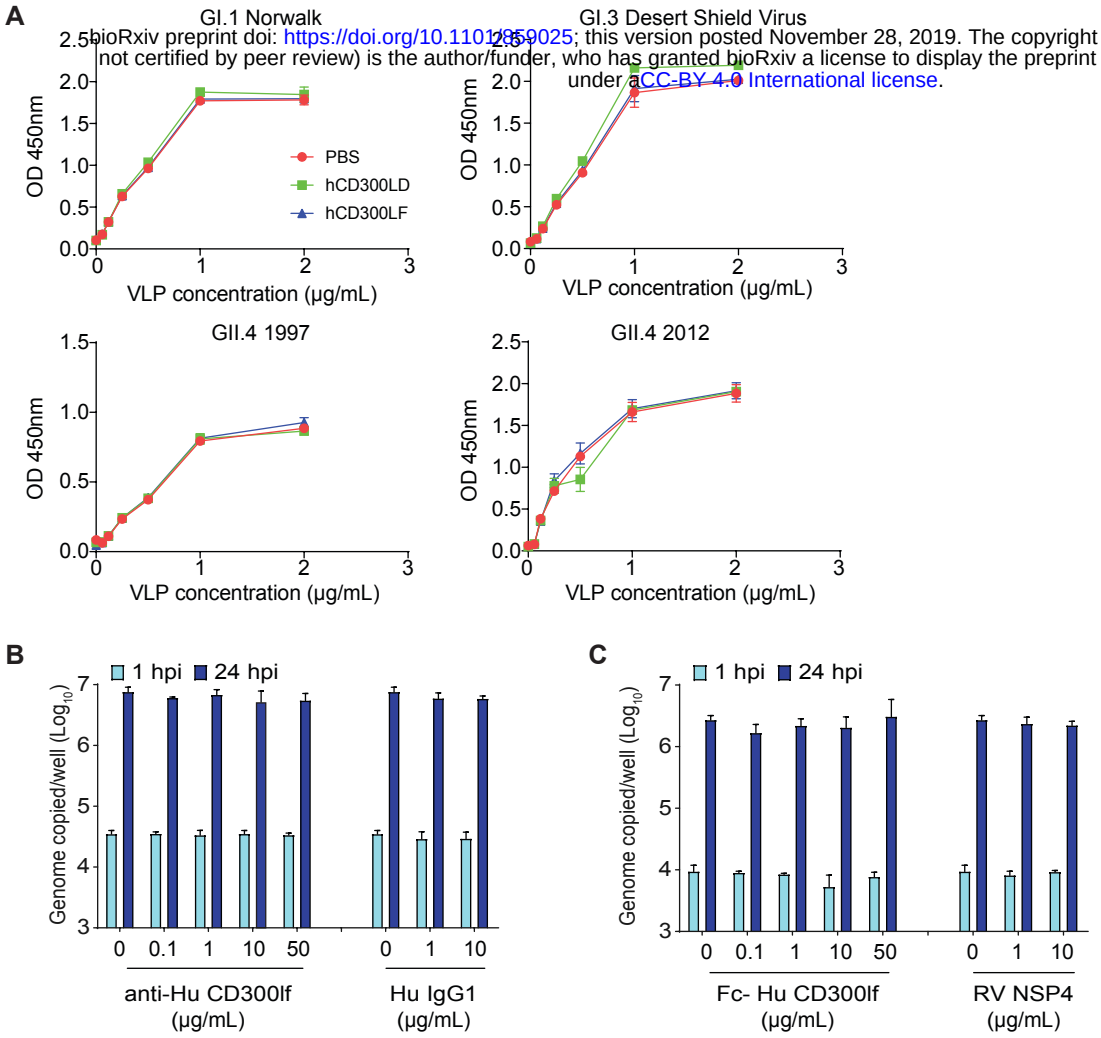

Figure 7. Human CD300lf is not a HNoV entry factor. (A) Human CD300lf and human CD300ld Fc-fusion proteins do not prevent binding of HNoV virus-like particles (VLPs) to pig gastric mucin for GI.1 Norwalk, GI.3 Desert Shield Virus, GII.4.1997, and GII.4.2012. (B) Polyclonal antibody against human CD300lf does not prevent HNoV GII.4 replication in HIEs relative to an IgG1 control. (C) Pre-incubating HNoV GII.4 with a human CD300lf Fc-fusion protein does not prevent HNoV replication in HIEs relative to a control protein (RV NSP4). Data in (A) is representative of at least two independent replicates each performed in duplicate. Data in (B and C) is pooled from three independent experiments with each condition and time point performed in triplicate wells of HIE cultures. Error bars represent standard deviation.

Figure S1

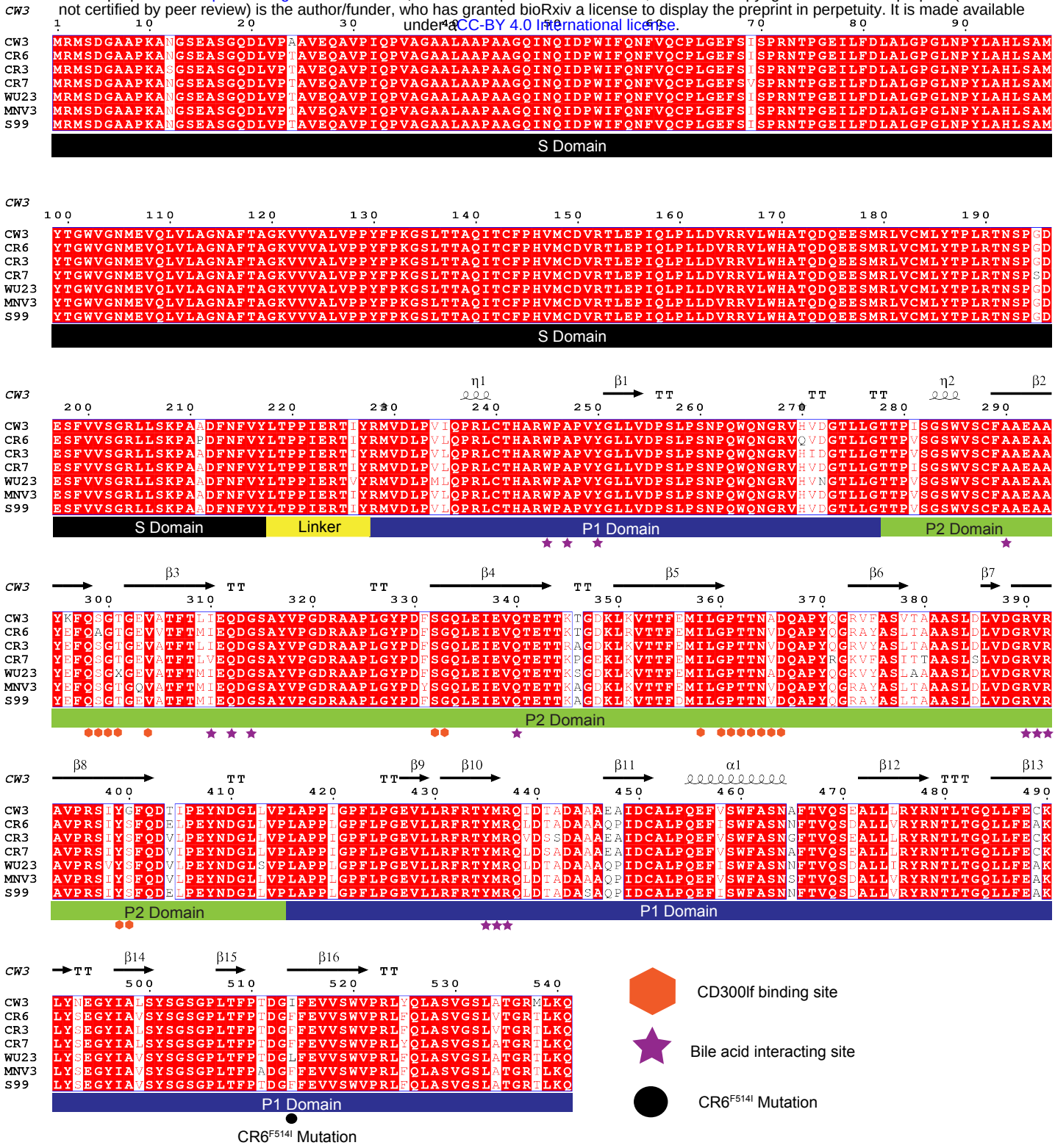

Figure S1. Tree and VP1 alignment showing CD300 interacting sites. VP1 is the major structural protein of MNoV and is comprised of a shell and protruding domain. The complete VP1 sequence of MNoV strains CW3, CR6, CR3, CR7, WU23, MNV3, and S99 were aligned. The VP1 shell domain comprises the core of the virion and is sufficient for virion assembly. The protruding domain mediates binding to CD300lf and bile salts and is comprised of discontinuous P1 and P2 subdomains. The CD300lf and secondary bile acid (GCDCA) binding sites are highlighted as is the F514I mutation which emerged during infection of Cd300lf-/-Stat1-/- mice13. Secondary structures labeled as alpha-helices (α), 310-helices (η), and beta-strands (β). The number following the annotation is the numerical order of that secondary structure. Helices are displayed as squiggles and strands are represented by a forward moving arrow under the annotation. TT = strict β-turns and TTT = strict α turns.